FP18 / FP38
Atmospheric Trace Gases

Institute of Environmental Physics
University of Heidelberg
Germany

Document Version: 08.10.2024

Compiled by Christoph Kern
Revised by Martin Horbanski, Tilman Hüneke, Marvin Knapp, Leonie Scheidweiler, Karolin
Voss, and Thomas Plewa

Safety Instructions

Before starting the experiment, students must be familiar with the laboratory regulations. A printed version of the regulations can be found next to the laboratory entrance. In particular, the following sources of hazard will be encountered during the course:

Nitrogen dioxide cuvette

For parts of the experiment a nitrogen dioxide (NO_2) cuvette with an NO_2 volume mixing ratio between 0.5 and 1.0% will be used. NO2 is harmful by inhalation. In case of nausea or respiratory tract irritation call a poison control center or doctor. In case of release of gas from the cuvette immediately leave the room and open windows if possible. Inform your experiment supervisor. Storage may only be carried out in well-ventilated areas. The cuvette must therefore be returned to an appropriate room after completion of the experiment.

Ethanol solution

Occasionally ethanol solution has to be applied to clean the optics in the telescope. If you need to clean any optical components please ask your tutor. The ethanol is stored safely in another room. Inhalation, eye and skin contact should be avoided. When working with it, wear protective gloves and eye protection. Keep the container away from any source of ignition and keep it tightly closed, if not in use. In case of contact with eyes, flush them with water for a few minutes. After swallowing drink plenty of water, then seek medical advice immediately.

Ultra violet (UV) radiation

In this experiment, a UV light source is used. UV radiation irritates and damages the eyes. Skin irritation and even severe burns can occur in case of continuous UV exposure. When working with the lightsource wear appropriate protective goggles. Do not look directly into the light. Avoid direct exposure of the skin. If possible, screen the optical setup. Do not use the light source longer than necessary.

Details on the listed hazards can be found in the information sheets attached to the laboratory regulations. By signing the 'Safety Briefing - Signature List', you confirm, that you have read and understood these instructions.

Overview

Differential Optical Absorption Spectroscopy (DOAS) is a widely used technique for the detection of atmospheric trace gases. It is based on the wavelength dependent absorption of light by atmospheric constituents. Various trace gases can be identified simultaneously by their spectral signatures which act as an individual 'fingerprint'. The DOAS technique has been implemented on several platforms: from ground, on aircrafts, balloons and satellites, and by using either artificial light sources, scattered sunlight, or direct sun- or moonlight.

Ground-based DOAS observations of scattered sunlight are very suitable both for long term measurements of atmospheric constituents and for measurements in the field using small portable instruments. The latter can be used, for example, to study emissions from volcanic plumes or the emission of reactive trace gases from remote salt lakes. Since those instruments are easy to maintain, they are ideally suited for the operation in remote regions with restricted technical infrastructure.

This experiment offers the opportunity to gain insight into spectroscopic remote sensing techniques, which are widely used to study the composition of the Earth's atmosphere. The DOAS method has been developed by U. Platt and D. Perner at the Institute of Environmental Physics of Heidelberg University. A relatively new application of this measurement technique is Multi-Axis DOAS (MAX-DOAS), which has an enhanced sensitivity for trace gases near the surface and allows to gain information on their vertical distribution.

The topics covered by this experiment are:

- To gain insight in the chemistry of the troposphere and stratosphere, in particular regarding ozone (O_3) and nitrogen dioxide (NO_2)

- To become familiar with spectroscopy and spectroscopic analysis techniques

- To gain insight into radiative transfer in the Earth's atmosphere

- To learn how to determine a trace gas concentration with DOAS

Instrumentation:

- Passive DOAS instrument with spectrograph/detector unit

- Quartz fiber

- Temperature regulator

- Halogen lamp

- Mercury vapor lamp

- Computer with measurement and analysis software

- Glass cell filled with NO_2

Study Guide

Before starting the experiment, please take the time to review these materials. While you do not need to know the exact step-by-step procedure of the experiment, you should be able to answer the following questions:

- How are O_3 and NO_2 distributed in the atmosphere? What are typical concentrations of these species? How do the concentrations vary with the time of day?

- What is the importance of O_3 in the stratosphere? What is the ozone hole? How is it formed?

- What is the importance of O_3 and NO_2 in the troposphere?

- What is the Beer-Lambert law of absorption? What does it describe?

- What does the word differential mean in Differential Optical Absorption Spectroscopy? Why is absolute absorption spectroscopy difficult to apply in the atmosphere?

- What components contribute to a measured spectrum?

- What equipment is necessary to record an atmospheric spectrum and why?

- What is a slant column density? What is a differential slant column density? What is a vertical column density?

- What is a Langley Plot? What is it used for?

- What knowledge is required in order to calculate trace gas concentrations from differential slant column densities?

- What is Multi-Axis DOAS? How can information about the vertical profile of a trace gas species be obtained with this technique?

Contents

Chapter 1

Background Information

1.1   The Atmosphere

Earth's atmosphere can be divided into layers. The most common classification is linked to the temperature. According to this scheme, the atmosphere is divided into the troposphere, the stratosphere, the mesosphere, the thermosphere and the exosphere. The regions dividing two layers are called 'pause', as in tropopause.

In the troposphere, the energy flow is dominated by incoming solar radiation heating up the surface (Figure 1.1). Sensible[1] and latent[2] heat are then transported from the ground up into the troposphere, and thermal energy is converted into potential energy. The updraft of an airparcel from the ground can be approximated by adiabatic cooling, which explains the temperature decline of $6\,\mathrm{K\,km^{-1}} - 10\,\mathrm{K\,km^{-1}}$. This transport of latent heat drives the weather in the troposphere and explains its turbulent behaviour. On the other hand, the energy balance in the stratosphere is dominated by radiative heating due to absorption of incoming radiation by trace gases, for example ozone (O_3). This leads to an increase of temperature with altitude and thus a stratification of the airmasses, hence the term 'stratosphere'.

1.2   Measurements and Dimensions

The concentration of a trace gas is the abundance of molecules in a volumetric unit. The abundance may be measured in number of molecules, where a commonly used unit is $\mathrm{molecules\,cm^{-3}}$. Another possibility is a mass concentration, for example in $\mathrm{\mu g\,m^{-3}}$.

The mixing ratio is the abundance of a trace gas relative to air. Commonly used units are ppm, ppb, and ppt. Sometimes, the quantity is related to the volume ratio, where the units ppmv, ppbv, and pptv may be used.

For DOAS measurements, the column density plays an important role. This is the concentration of a species integrated along a light path and is typically measured in $\mathrm{molecules\,cm^{-2}}$. Depending on the light path, this is called slant column density (SCD), or vertical column density (VCD). For O_3, the Dobson Unit[3] (DU) has become popular. $100\,\mathrm{DU}$ correspond to an O_3 VCD of $1\,\mathrm{mm}$ at $0\,^{\circ}\mathrm{C}$ and $1013.25\,\mathrm{hPa}$. Typical O_3 VCDs in the atmosphere are $300\,\mathrm{DU} - 400\,\mathrm{DU}$. Therefore, the total O_3 in the atmosphere corresponds to a layer with $3\,\mathrm{mm} - 4\,\mathrm{mm}$ thickness when brought to normal conditions.

---

[1]Thermal energy that can be measured with a thermometer.

[2]Energy originating from evaporation on the ground or in the ocean.

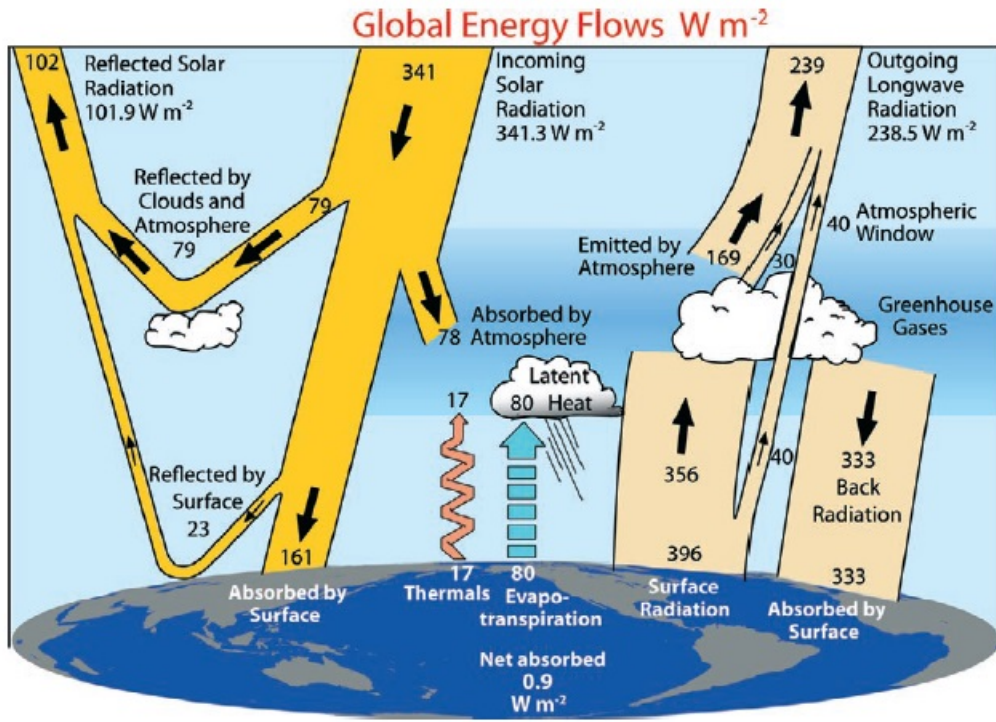[3]$1\,\mathrm{DU} = 2.6 \times 10^{16}\,\mathrm{molecules\,cm^{-2}}$

Figure 1.1: Global annual mean energy budget. ([30])

1.3 Composition of Air

The main constituents of air are oxygen (O_2), nitrogen (N_2), and argon (Ar) (see Table 1.1). Water vapor (H_2O) can have concentrations of 0.02% – 2.5% in the troposphere. In the stratosphere, the mixing ratio of water vapor is only about $3\,ppm$ – $4\,ppm$. All other gases together make up only 0.04% and are therefore called trace gases. Regarding the stable main constituents, the atmosphere is well-mixed and the number concentrations are basically proportional to the atmospheric pressure profile. In first approximation, atmospheric pressure decreases exponentially with altitude, approximately with a surface pressure of $1013\,hPa$ and a scale height of $8\,km$. In contrast to the main constituents, trace gas concentrations are significantly affected by complex production and destruction cycles and may therefore vary strongly within space and time.

O_4

The O_4 molecule is the dimer of the oxygen molecule O_2. It can be formed when two oxygen molecules collide. Therefore, its concentration is proportional to the square of the oxygen concentration in the atmosphere. For this reason, its column is given in $molecules^2\,cm^{-5}$. Its vertical profile is an exponential decrease with altitude with a scale height of approximately $4\,km$. Since the vertical profile of O_4 concentration is well known, the measured column densities can be used to gain insight into photon paths in the atmosphere, i.e. light path enhancement due to aerosols and clouds [33].
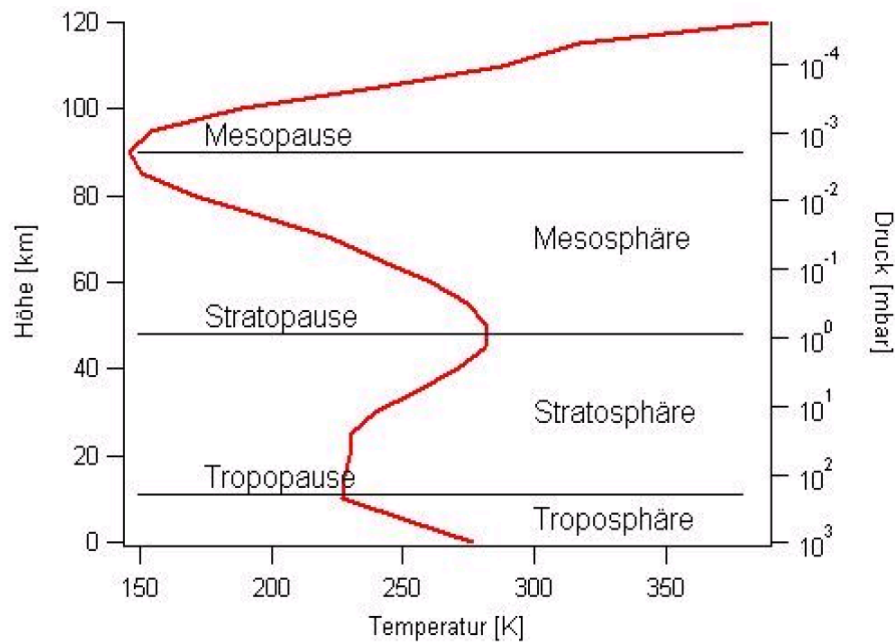
Figure 1.2: Atmospheric temperature profile and layering.

Table 1.1: Chemical makeup of the atmosphere. ()

Volume Fraction	Symbol	Gas
78.084 %	N_2	Nitrogen
20.947 %	O_2	Oxygen
0.934 %	Ar	Argon
up to 4 %	H_2O	Water vapor
0.035 %	CO_2	Carbon Dioxide
18.182 ppm	Ne	Neon
1.70 ppm	CH_4	Methane
1.14 ppm	Kr	Krypton
0.53 ppm	H_2	Hydrogen
0.31 ppm	N_2O	Nitrous Oxide
0.10 ppm	CO	Carbon Monoxide
0.07 ppm	O_3	Ozone
≈ 4 ppb		Chloroflourocarbons (CFCs)

Chapter 2

Atmospheric Chemistry I: Stratospheric Ozone

2.1 The Importance of Ozone in the Stratosphere

The ozone molecule (O_3) is composed of three oxygen atoms. In its gas phase, it is light blue. At $-111.9\,°C$, it condensates to an explosive, dark blue, magnetic liquid. At $-192.5\,°C$, it crystalizes to a dark violet mass. The dissociation at room temperature is slow, while it occurs explosively if heated.

The average lifetime of an O_3 molecule at an altitude of $25\,km$ is about $1\,h$. This lifetime is determined by its photolysis frequency. However, the O_3 concentration of a given airmass changes slowly with time, as most oxygen atoms originating from ozone photolysis quickly react back to O_3 (see Section 2.2). Therefore, it usually takes months or years to significantly change the O_3 concentration in a given airmass. This stands in contrast to the quick reduction seen in the ozone hole formation discussed in Section 2.2.4.

O_3 is a highly efficient absorber of UV radiation. The largest absorption of photons by O_3 occurs between $240\,nm$ – $310\,nm$. Even though it is present only in small concentrations, it blocks $95\,\%$ – $99\,\%$ of the harmful UV radiation ($\lambda < 320\,nm$) at an altitude of $20\,km$ – $50\,km$, as Figure 2.1 shows. Therefore, the ozone layer is of great importance for life on Earth.

2.1.1 Vertical Profile of Ozone Concentration

About $90\,\%$ of the total O_3 column is located in the stratosphere, the rest in the troposphere. In mid latitudes, the O_3 concentration at the ground is about $1 \times 10^{12}\,molecules\,cm^{-3}$, while typical concentrations in the stratosphere are $1 \times 10^{13}\,molecules\,cm^{-3}$ – $2 \times 10^{13}\,molecules\,cm^{-3}$ (see Figure 2.2, left panel). The vertical profile of O_3 is determined by the number of UV photons and the decreasing number of O_2 molecules in the upper atmosphere. At high altitudes, the air is so thin that the UV photons barely ever hit O_2 molecules and no atomic oxygen is formed. As the air density increases at lower altitudes, the probability for oxygen photolysis increases, which causes more O_3 to be formed. The lower end of the ozone layer is reached when no more UV photons necessary for the formation of O_3 are available, as they have all been absorbed in higher layers.

2.1.2 The Effects of Harmful UV Radiation

The energy of shortwave UV radiation with wavelengths below $320\,nm$ is enough to destroy molecules, including proteins and amino acids, which are the main constituents of organic
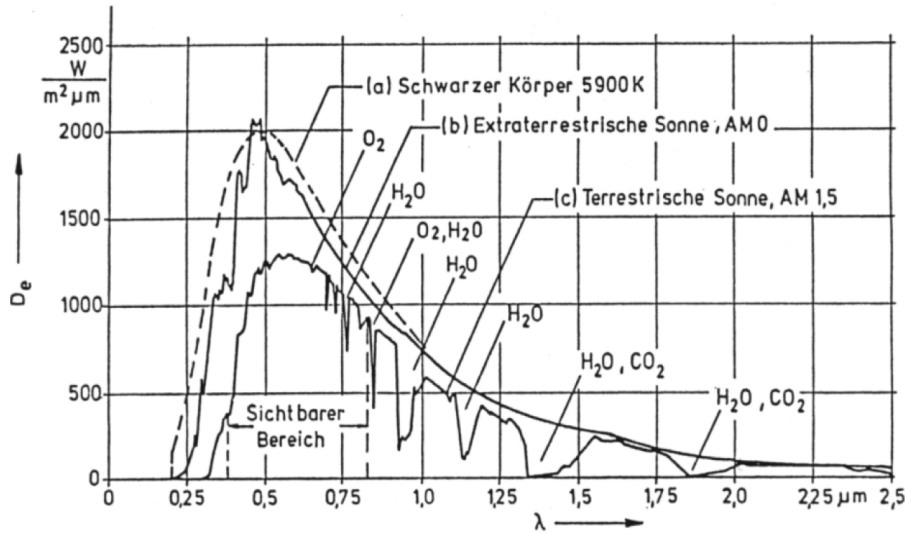
Figure 2.1: Spectrum of incident solar radiation at the top of the atmosphere and at sea level.
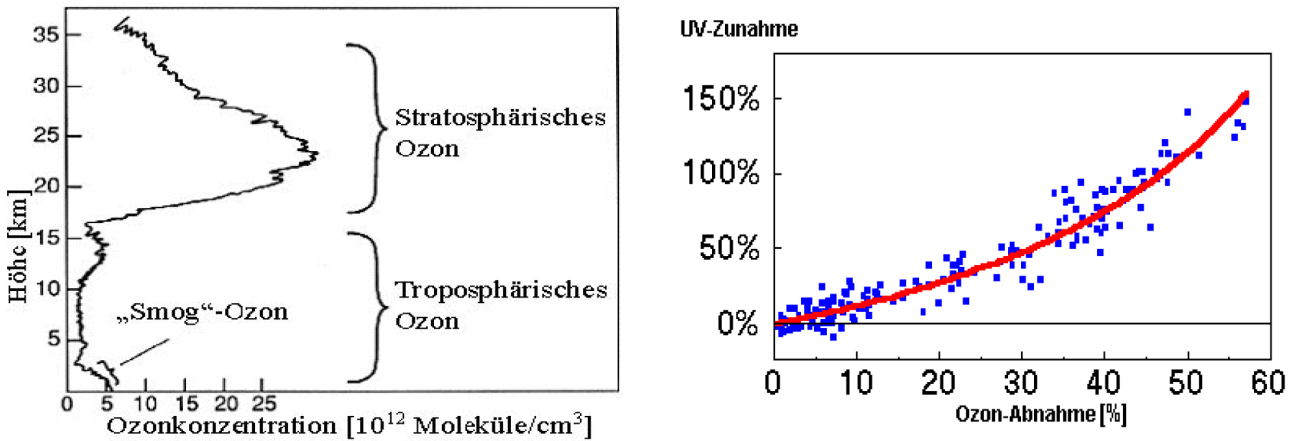
Figure 2.2:   Left: O_3 concentration vertical profile. Right: The enhancement of harmful UV radiation is exponential with decreasing O_3 columns, as described by the Beer-Lambert law of absorption. This plot shows data measured in Antarctica between February 1991 and December 1992.

matter. Enhanced UV radiation directly increases the risk of skin cancer and biological mutation, and has even been shown to directly influence marine biology and agriculture (see e.g. [12, 28, 29, 35]). A decreasing O_3 column in the stratosphere enables more UV radiation to reach Earth's surface. This relationship is not linear, as shown in Figure 2.2, right panel.

2.2   Photochemistry of Ozone in the Stratosphere

2.2.1   Chapman Cycle

In 1930, Sydney Chapman [3] published the first simple theory about O_3 in the stratosphere. He postulated O_3 to be the result of a chemical equilibrium of 4 photochemical reactions. At altitudes from $20\,\text{km} - 25\,\text{km}$, atomic oxygen is formed during the photolysis of O_2 by shortwave UV radiation ($\lambda < 242\,\text{nm}$).

$$O_2 + h\nu \longrightarrow 2\,O \tag{2.1}$$

O_3 is then formed by the recombination of the atomic oxygen with molecular oxygen.

$$O_2 + O + M \longrightarrow O_3 + M \tag{2.2}$$

M is a chemically neutral molecule (e.g. N_2 or O_2) needed for conservation of momentum. To reach an equilibrium O_3 concentration, ozone destruction reactions are also necessary. Chapman held the photolytic dissociation by photons with a wavelength of $\lambda < 1100\,\mathrm{nm}$ of O_3 responsible.
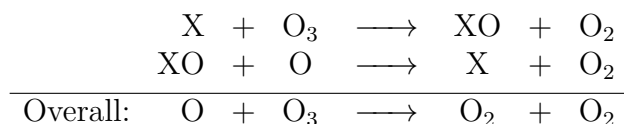
$$O_3 + h\nu \longrightarrow O_2 + O(^3P) \tag{2.3}$$

The formed oxygen atoms then either react according to Equation 2.2 and form O_3 again, or they destroy an additional O_3 molecule.

$$O_3 + O \longrightarrow 2\,O_2 \tag{2.4}$$

These four reactions comprise the Chapman cycle. The mechanism postulated by Chapman was correct, but incomplete. The measured O_3 columns were always lower than his prediction, usually by about 40 %. Additionally, the predicted altitude of the maximum O_3 concentration was incorrect.

2.2.2 Catalytic Ozone Destruction

Today, we know that catalytic reactions play an important role in the destruction of O_3. These reactions are enabled by a catalist X, a molecule that is required during the reaction, but remains unchanged after the reaction. They accelerate the O_3 destruction previously mentioned in Equation 2.4. For the Chapman cycle, typical catalists include the groups HO_x (H, OH, HO_2), NO_x (NO, NO_2), ClO_x (Cl, ClO), and BrO_x (Br, BrO).

$$
\begin{array}{rcccccc}
& X & + & O_3 & \longrightarrow & XO & + & O_2 \\
& XO & + & O & \longrightarrow & X & + & O_2 \\
\hline
\text{Overall:} & O & + & O_3 & \longrightarrow & O_2 & + & O_2
\end{array}
$$

As catalysts are not removed from the cycle, they are available for further O_3 destruction. HO_x and NO_x can cycle through this reaction scheme $1000 - 10\,000$ times before they are removed from the atmosphere through chemical reaction or sedimentation. Since these reactions are much faster than the reaction of O_3 with O, the catalysts have a strong influence on the chemistry of stratospheric O_3. By taking these catalytic reactions into account, the predicted O_3 concentrations decreased and for the first time it was possible to match predicted and measured vertical O_3 profiles (see Figure 2.3, left panel).

2.2.3 Anthropogenic Influence on the Total Ozone Column

Ever since the mid 80s, the average global total O_3 columns have been decreasing. The total O_3 decrease after considering natural variations is about 5 % per decade (see Figure 2.3, right panel). This decrease can be seen in mid latitudes, and is not restricted to the regions over Antarctica affected by the ozone hole (see Section 2.2.4). O_3 destruction by chlorofluorocarbons (CFCs) was detectable as early as 1974. These gases are industrially produced compounds containing carbon (C), fluorine (F) and chlorine (Cl). They found widespread use as cooling agents and gas propellants in spray cans by the 1950s. CFC molecules are chemically inert in the lower troposphere. However, upon reaching the upper area of the ozone layer at an altitude of about 30 km, CFCs are photolyzed by shortwave UV radiation, contributing to catalytic O_3
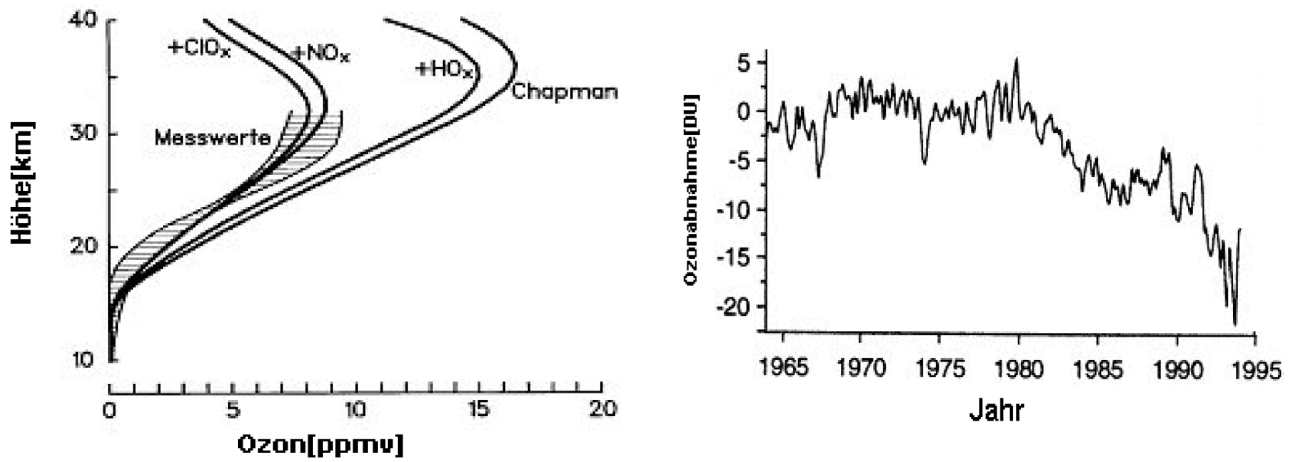
Figure 2.3: Left: The Chapman cycle alone predicts O_3 mixing ratios approximately twice as high as the measured values. Only by taking the catalytic ozone destruction into account the measurements could be understood. Right: Decrease in global O_3 after removing all known natural variations.
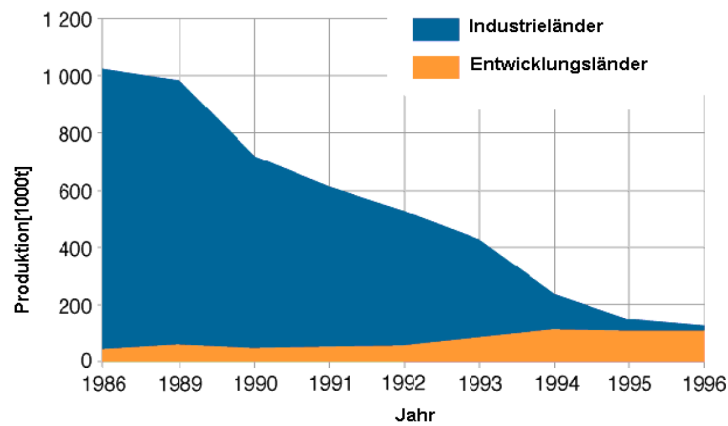

Figure 2.4: Global CFC production by year for industrialized and developing nations.

destruction. Through this process, the Cl concentration in the atmosphere was increased by a factor of 6 within a few decades.

By the mid-1980s, scientists realised the influence of CFCs on O_3 destruction. In 1987, the industrialized nations signed the Montreal Protocol to reduce CFC emissions, followed by several additional treaties thereafter. Figure 2.4 shows the global CFC production between 1986 and 1996.

Due to the long lifetimes of CFCs in the atmosphere (up to 100 years for some species), they continue to act as catalysts in O_3 destruction even though emissions have been drastically reduced. In very recent years, the measured ozone hole has seemed to decrease in size and intensity. However, it will still take several decades for the ozone layer to recover.[1]

2.2.4 The Ozone Hole

In the middle of the 1980s, scientists predicted that the maximum O_3 loss due to destruction by CFCs would be 10 %. However, in October of 1984, more than 40 % of the O_3 in the ozone layer above Antarctica were destroyed.

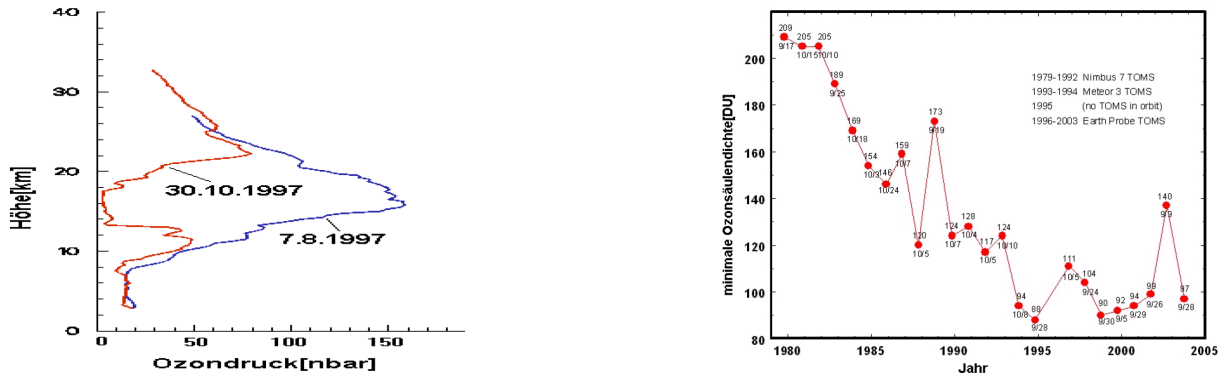[1] For details, see *Scientific Assessment of Ozone Depletion, WMO, 2010* at www.wmo.int

Figure 2.5: Left: Altitude profile of the ozone concenration measured over Antarctica in August 1997 and October 1997. Right: Time series of the annual minimum of the measured ozone column density.

At the end of August, the O_3 column over Antarctica decreases rapidly. It reaches a minimum in September. In November, the values increase back to normal levels.

O_3 is destroyed only in the altitude range of 12 km – 30 km, as shown in Figure 2.5. However, this is also where the ozone layer is normally located. These findings could not be explained by dynamic processes alone. Instead, a complex chemical mechanism was found to be responsible. Cl and Br reach the polar stratosphere in the form of transport-gases such as CFCs. Here, they react to so-called reservoir gases, which binds the molecules and removes from from ozone-destroying reactions. During the polar night, a combination of two processes then combine to again release these halogens.

For one, a polar vortex forms in the stratosphere. Tropical air masses are transported towards the poles and are deflected by the coriolis force. The large temperature gradient present in the Antarctic winter from July to October causes the air to swirl around the south pole in a stable stratospheric vortex, effectively shielding the south pole from other adjacent air masses. In the absence of sunlight, the air in the Antarctic stratosphere then cools to temperatures around $-80\,°C$. At these very low temperatures, a second phenomenon takes place. So-called Polar Stratospheric Clouds (PSC) are formed from ice, nitric acid, and some sulfuric acid. The extreme conditions necessary to form such clouds are only present during the Antarctic winter in the absence of sunlight in altitudes between 15 km - 25 km. Once formed, the PSCs very effectively activate halogens through the following heterogeneous reactions taking place on the ice surfaces.

$$XONO_2 + H_2O \longrightarrow HNO_3 + HOX \tag{2.5}$$
$$XONO_2 + HX \longrightarrow HNO_3 + X_2 \tag{2.6}$$
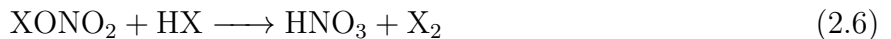
with $X = \{Cl, Br\}$.

Without the PSC surfaces, these reactions would be very slow and therefore irrelevant. When the Sun rises in the Antarctic spring, the activated halogens act very effectively as catalysts for ozone destruction. In the Arctic, the distribution of land masses prevents the formation of a very strong polar vortex, therefore Arctic ozone hole is much less pronounced than the Antarctic version. If all conditions remain the same, the ozone layer should recuperate by the middle of the coming century. However, some aspects are still poorly understood. For example, when ozone absorbs UV radiation, it heats the stratosphere. Ozone depletion therefore leads to a cooling trend in the stratosphere, which could lead to an increased abundance of PSCs and therefore even stronger ozone destruction. These and other questions are still being explored to date.

Chapter 3

Atmospheric Chemistry II: Nitrogen Oxides

The Nitrogen oxides NO (nitric oxide) and NO_2 (nitrogen dioxide) are together referred to as NO_x. They are one of the most problematic pollutants in urban areas not only in developing, but also in industrialised countries. They are key species in the control of tropospheric O_3 production and by this play an important role in the formation of the so-called Los Angeles Smog (Section 3.4). Moreover, the concentration of NO_x has a strong influence on the atmospheric level of hydroxyl radicals (OH), which initiates the degradation of most oxidizable trace gases [7].

3.1 Health Aspects of NO_2 Air Pollution

NO_2 is a brown, toxic gas. Mixing ratios over 20 ppm cause strong irritations of the respiratory system including tickling of the throat, headaches, dizziness, and eventually nausea. At higher mixing ratios, it can lead to death, 700 ppm after 30 minutes are lethal. Inhaled gas together with the humid mucosae creates nitric acid (HNO_3), which causes strong degradation of the lungs capillaries (Air Liquide EG-safety data sheet). In addition to being a health hazard in itself, NO_2 is a precursor of a number of harmful secondary pollutants, including the formation of inorganic particulate matter via HNO_3, and photo oxidants (e.g. O_3 and PANs[1]). These relationships are shown in Figure 3.1.

3.2 Sources and Sinks of Tropospheric NO_x

The global emissions of NO_x are caused by both human activities and natural processes. Table 3.1 shows the sources of NO_x and their contributions to the global emissions.

New highly resolved satellite measurements allow to determine the global distribution of these NO_x sources. Figure 3.2 depicts the 18 month mean of a satellite measurement of NO_2, which was recorded by the SCIAMACHY instrument aboard the ESA satellite ENVISAT. Areas with high VCDs correlate with urban areas and therefore also with anthropogenic sources. In fact, more than half of the global NO_x emissions are man-made.

The major source of anthropogenic NO_x is the combustion of fossil fuels in industrial processes, power plants, and traffic. The most important mechanism for natural and anthropogenic production of NO_x is the Zel'dovic cycle [38] which describes the formation of thermal NO. The term thermal is chosen due to the high activation energy necessary for Reaction 3.2 of
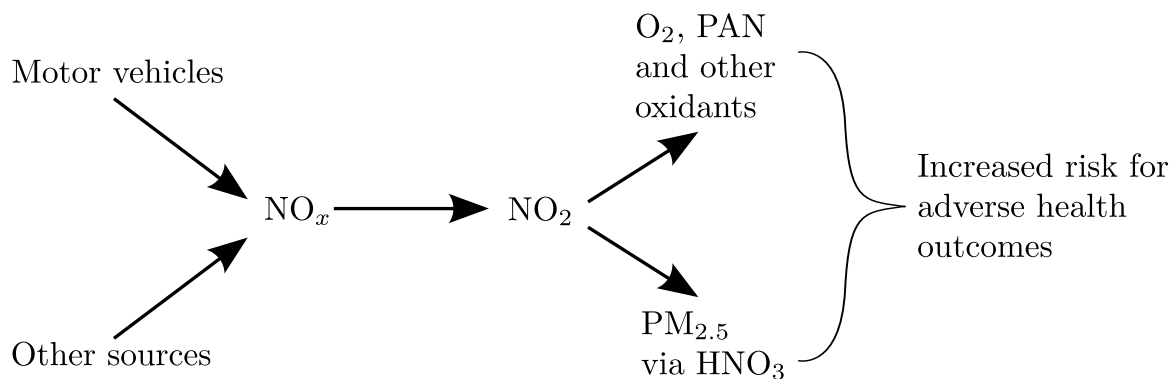
---

[1]peroxyacyl nitrates

Figure 3.1: Simplified relationship of NO_x emission with formation of NO_2 and other harmful reaction products including O_3 and particulate matter ($PM_{2.5}$) [36].

$318\,kJ\,mol^{-1}$. Therefore, NO is emitted from combustion processes, e.g. in combustion engines (traffic) and from thermal power plants or other industrial combustion processes.

$$O_2 + M \longrightarrow O + O + M \tag{3.1}$$
$$O + N_2 \rightleftharpoons NO + N \tag{3.2}$$
$$N + O_2 \rightleftharpoons NO + O \tag{3.3}$$
$$N + OH \rightleftharpoons NO + H \tag{3.4}$$

Afterwards, NO_2 can be produced via Reaction 3.7. NO_x is removed from the atmosphere mainly by further oxidation. During the day, hydroxyl radicals oxidize NO_2 to HNO_3, which is then removed from the atmosphere by wet (acid rain) and dry deposition:

$$NO_2 + OH + M \longrightarrow HNO_3 + M \tag{3.5}$$

Another sink of NO_x is the reaction of NO_2 with O_3. Although the rate coefficient for this reaction is relatively small, it cannot be neglected in areas with high O_3 concentrations in the absence of sunlight. During daytime, this reaction plays no role because NO_3 is rapidly photolyzed. During the night, NO_3 reacts with NO_2 to form the anhydrite of nitric acid N_2O_5. The major sink of tropospheric N_2O_5 is hydrolysis and subsequent wet or dry deposition [19].

3.3 Photostationary State with Ozone

NO_2 is mainly a secondary pollutant. The oxidation to NO_2 is explained by [16].

Table 3.1: Summary of the main anthropogenic and natural sources for global tropospheric NO_x. Taken from e.g. [15].

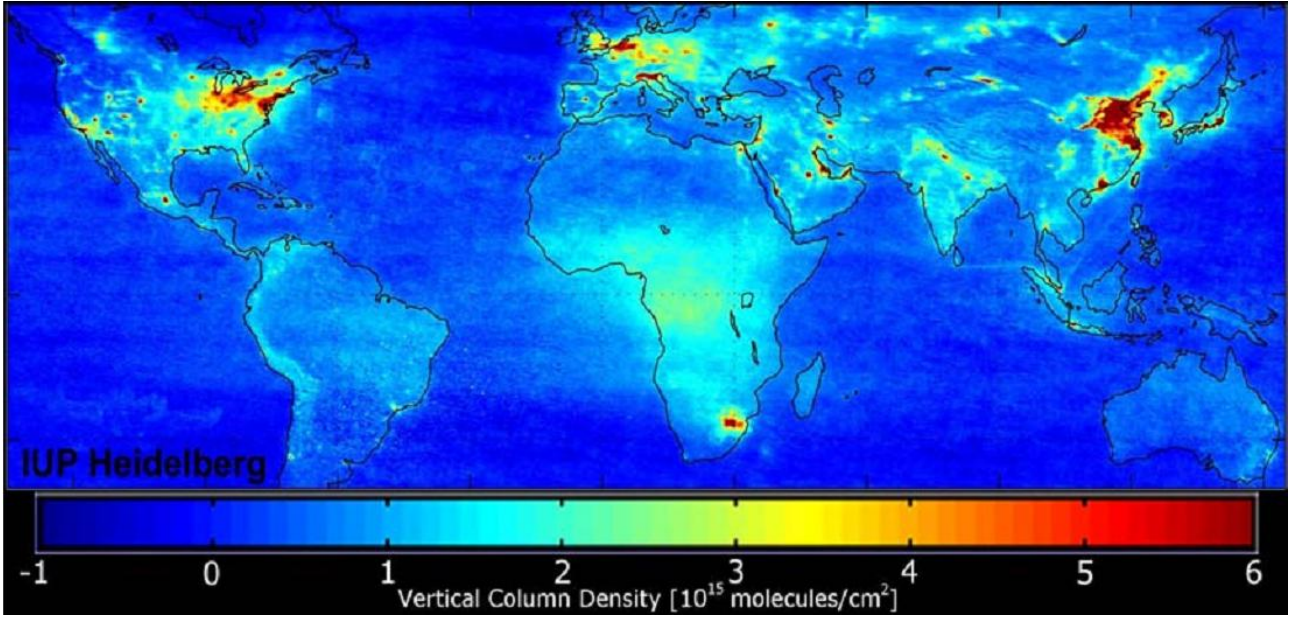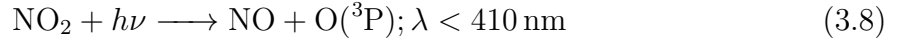| Sources	Emission / $Mt\,yr^{-1}$	Range of Uncertainty / $Mt\,yr^{-1}$
Fossil fuel combustion	22	13-31
Biomass burning	7.9	3-15
Soil microbial production	7.0	4-12
Lightning	5.0	2-20
Aircraft	0.8	0.59-0.95
Stratospheric	0.64	0.4-1
Total	44	23-81

Figure 3.2: Satellite measurement of the NO_2 VCD averaged over the time period from January 2003 to June 2004. The measurements have been performed with the SCIAMACHY instrument aboard the ESA satellite ENVISAT. [1].

$$O(^3P) + O_2 + M \longrightarrow O_3 + M \tag{3.6}$$

$$O_3 + NO \rightleftharpoons NO_2 + O_2 \tag{3.7}$$

$$NO_2 + h\nu \longrightarrow NO + O(^3P); \lambda < 410\,\text{nm} \tag{3.8}$$

The third reaction partner in Reaction 3.6 is required due to conservation of momentum. The photolysis in Reaction 3.8 only occurs at wavelengths below 410 nm.

The steady state concentrations of O_3, NO, and NO_2 are linked by the Leighton ratio:

$$\frac{[NO]}{[NO_2]} = \frac{j_{NO_2}}{k_{O_3+NO} \cdot [O_3]} \tag{3.9}$$

k_{O_3+NO} is the reaction constant for Equation 3.7. Since the photolysis rate changes with the SZA, the Leighton ratio also changes during the course of the day. At noon of a clear day, when the photolysis rate has its maximum of $j_{NO_2} \approx 8 \times 10^{-3}\,\text{s}^{-1}$, the Leighton ratio has its maximum and the lifetime of NO_2 is about 2 min. At typical O_3 mixing ratios of 30 ppb, $\frac{[NO]}{[NO_2]}$ is on the order of 1.

3.3.1 NO₂ Diurnal Cycle

In an atmosphere that is free of volatile organic compounds (VOCs), NO_2, NO and O_3 are in a self-contained diurnal cycle that is strongly dependent on the Sun's UV light. In the morning, the intensity of solar light increases. This leads to photodissociation of NO_2. During the day, NO and NO_2 are in a photostationary balance (see Reactions 3.6 to 3.8).

Due to the dissociation of N_2O_5 to NO_2, the statospheric mixing ratio of NO_2 increases during the day.

$$N_2O_5 + h\nu \longrightarrow NO_2 + NO_3 \tag{3.10}$$

NO_3 rapidly splits up to form either NO_2 or NO. This only happens during the daytime.

$$NO_3 + h\nu \longrightarrow NO + O_2 \tag{3.11}$$
$$NO_3 + h\nu \longrightarrow NO_2 + O \tag{3.12}$$

In the evening, the photolysis decreases and Reaction 3.8 no longer creates NO. The result is an increase of NO_2. At night, NO_2 forms N_2O_5 again.

$$NO_2 + O_3 \longrightarrow NO_3 + O_2 \tag{3.13}$$
$$NO_3 + NO_2 + M \longrightarrow N_2O_5 + M \tag{3.14}$$

3.4 Photochemical Smog / Deviation from the Photostationary State

Since the first reports of photochemical smog in Los Angeles in the late 1940's, extremely high O_3 levels have been measured in urban areas throughout the whole world. In Mexico City, O_3 levels over 400 ppb have been reported. Photochemical smog is worst when high levels of volatile organic compounds (VOCs) and NO_x are emitted into a thermal inversion layer, trapping them closely to the ground, and irradiated by sunlight during transport to downwind regions. This section discusses the mechanisms responsible for the creation of photochemical smog.
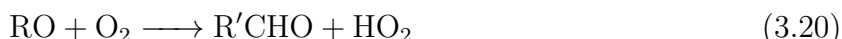
The Leighton relation is only valid if Reactions 3.6 to 3.8 describe the major sources and sinks of NO_2 and O_3. In the presence of VOCs, another reaction path for the conversion of NO to NO_2 exists which does not include the destruction of O_3. The OH radical which usually initiates the reaction chain is mainly formed by means of ozone photolysis:

$$O_3 + h\nu \longrightarrow O(^1D) + O_2; \lambda < 320\,\text{nm} \tag{3.15}$$
$$O(^1D) + H_2O \longrightarrow 2\,OH \tag{3.16}$$
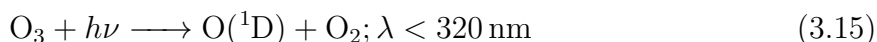
The reaction chain is started by the oxidation of a hydrocarbon (RH), which may be described as

$$RH + OH \longrightarrow R + H_2O \tag{3.17}$$
$$R + O_2 \longrightarrow RO_2 \tag{3.18}$$

The peroxy radicals RO_2 and HO_2 react with NO and produce NO_2 without destroying O_3 (see e.g. [2, 4, 20]).

$$RO_2 + NO \longrightarrow NO_2 + RO \tag{3.19}$$
$$RO + O_2 \longrightarrow R'CHO + HO_2 \tag{3.20}$$
$$HO_2 + NO \longrightarrow NO_2 + OH \tag{3.21}$$

This scheme can be applied multiple times until the initial VOC is converted to CO_2 or CO and H_2O. Together with the Reactions 3.6 to 3.8, this can be written as an effective equation for the O_3 production:

$$RH + 4\,O_2 + 2\,h\nu \longrightarrow R'CHO + H_2O + 2\,O_3; \lambda < 410\,\text{nm} \tag{3.22}$$
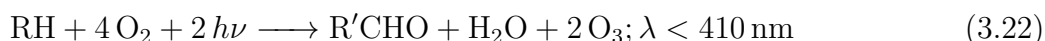
The reaction system is illustrated in Figure 3.3 together with the most important sources of OH, hydroxyl, and peroxy radicals.
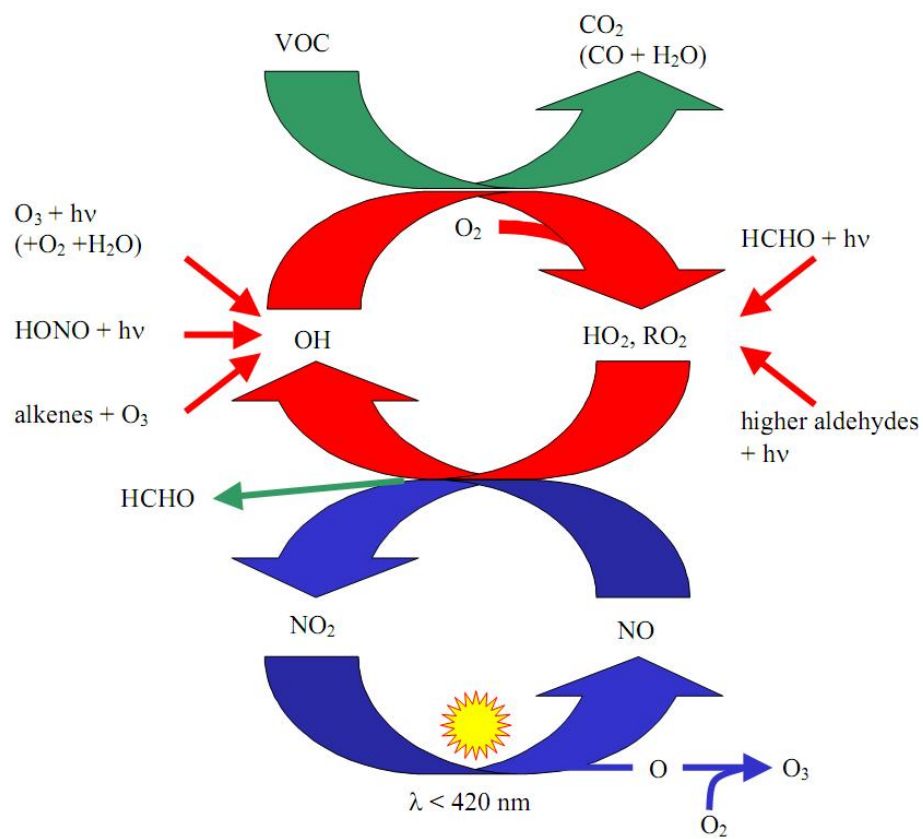
Figure 3.3: Reaction cycles of tropospheric NO_x and O_3 in a polluted atmosphere. The photostationary state of NO_x is illustrated by the blue cycle. It is disrupted by the presence of VOCs, which results in a net production of O_3. [31]

Chapter 4

DOAS

Differential Optical Absorption Spectroscopy (DOAS) is a widely used technique in atmospheric research for the detection of numerous trace gases, such as O_3, NO_2, formaldehyde, halogen radicals (BrO, IO), H_2O, and many others [21, 22]. This chapter will cover an approximative radiative transfer model for the application to the DOAS method.

4.1   The Beer-Lambert Law

When electromagnetic radiation passes through matter, its intensity is modified. For this experiment, the dominant processes are absorption and scattering. These are extinction processes, meaning they reduce the intensity of radiation. This reduction depends on the wavelength of light and the amount of matter it travels through, and is described by the Beer-Lambert law. Let $I_0(\lambda)$ be the intensity of a light beam at wavelength λ before entering the medium and $I(\lambda)$ be the intensity after passing through it. Then the relationship between incident and transmitted intensity is

$$I(\lambda) = I_0(\lambda) \cdot \exp\left(-\tau(\lambda)\right) \tag{4.1}$$

$$= I_0(\lambda) \cdot \exp\left(-\sigma(\lambda) \cdot \rho \cdot L\right), \tag{4.2}$$

where τ is the optical density, σ is the extinction cross-section and ρ is the concentration of the trace gas, and L is the length of the layer the light passed through. In general, σ depends on pressure and temperature along the light path. Furthermore, the concentration along the light path can vary. The Lambert-Beer law describes the absorption for N different absorbers i through

$$I(\lambda, L) = I_0(\lambda) \cdot \exp\left(-\int_0^L \sum_{i=1}^{N} \sigma_i(\lambda) \cdot \rho_i(s) \, \mathrm{d}s\right). \tag{4.3}$$

4.2   The DOAS Method

To determine the concentration of a particular trace gas in the atmosphere, it would, in principle, be necessary to quantify all factors influencing the intensity $I(\lambda)$ of a spectrum of light. In the laboratory, this can be achieved by removing the absorber from the light path. In the atmosphere, however, where this is impossible, the multiple factors influencing the intensity pose a dilemma. DOAS overcomes this challenge by using the fact that many processes in radiative transfer show broad or even smooth spectral characteristics, while certain trace gases
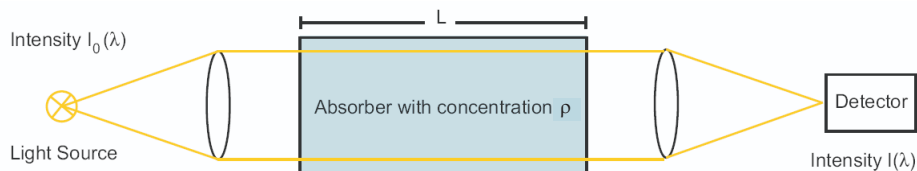
Figure 4.1: Light with the initial intensity $I_0(\lambda)$ is emitted by a light source. After passing through a volume of air containing an absorber with concentration ρ, the detector measures the reduced intensity $I(\lambda)$.

exhibit narrowband absorption structures. The basic principle of DOAS is thus the separation of spectral structures in narrowband (varying strongly with wavelength) and broadband (varying slowly with wavelength) components in differential spectra, so that changes in narrowband absorptions can be detected (illustrated in Figure 4.4). To use Equation 4.3 in DOAS measurements, it therefore has to be modified according to properties of radiative transfer in the atmosphere and the measurement principles of DOAS instruments.

4.2.1 Narrowband Components

Fraunhofer Reference Spectrum

The Sun's spectrum is highly structured (see Figures 2.1 and 4.3, top). These structures must be taken into account in a DOAS retrieval when using a passive instrument, i.e. when using the Sun as a light source. This is usually achieved by using a so-called Fraunhofer reference spectrum $I_0(\lambda)$, which is a solar spectrum recorded under conditions in which the investigated trace gases show little or no absorption.

Trace Gas Absorption

The primary quantity measured by DOAS instruments is the slant column density (SCD). The SCD which we denote as $S_i(\lambda)$ is defined as

$$S_i(\lambda) = \int_0^L \rho_i(s)\mathrm{d}s\,. \tag{4.4}$$

It is an integrated quantity and has the units molecules cm^{-2}.
Each trace gas has its individual absorption cross-section σ_i which serves as a spectral fingerprint. Several trace gases can be measured simultaneously even if their absorption features are superimposed (see Figure 4.2). By fitting these cross-sections to recorded differential spectra, SCDs are retrieved for each gas individually.
If the Fraunhofer reference spectrum already contains absorption of a trace gas, the SCD is often called differential Slant Column Density (ΔSCD or ΔS).

$$\Delta S_i = S_i - S_{0,i}\,, \tag{4.5}$$

where S_0 is the SCD of the Fraunhofer reference spectrum containing its extinction effects.

The Ring Effect

In 1961, J. Grainger and J. Ring [11] discovered that the the depth of the Fraunhofer lines was smaller when examining scattered sunlight than when direct sunlight is observed. This was attributed to inelastic rotational Raman scattering [32], which slightly changes the wavelength of the scattered photon when the scattering occurs. This causes a "filling in" of strong absorption
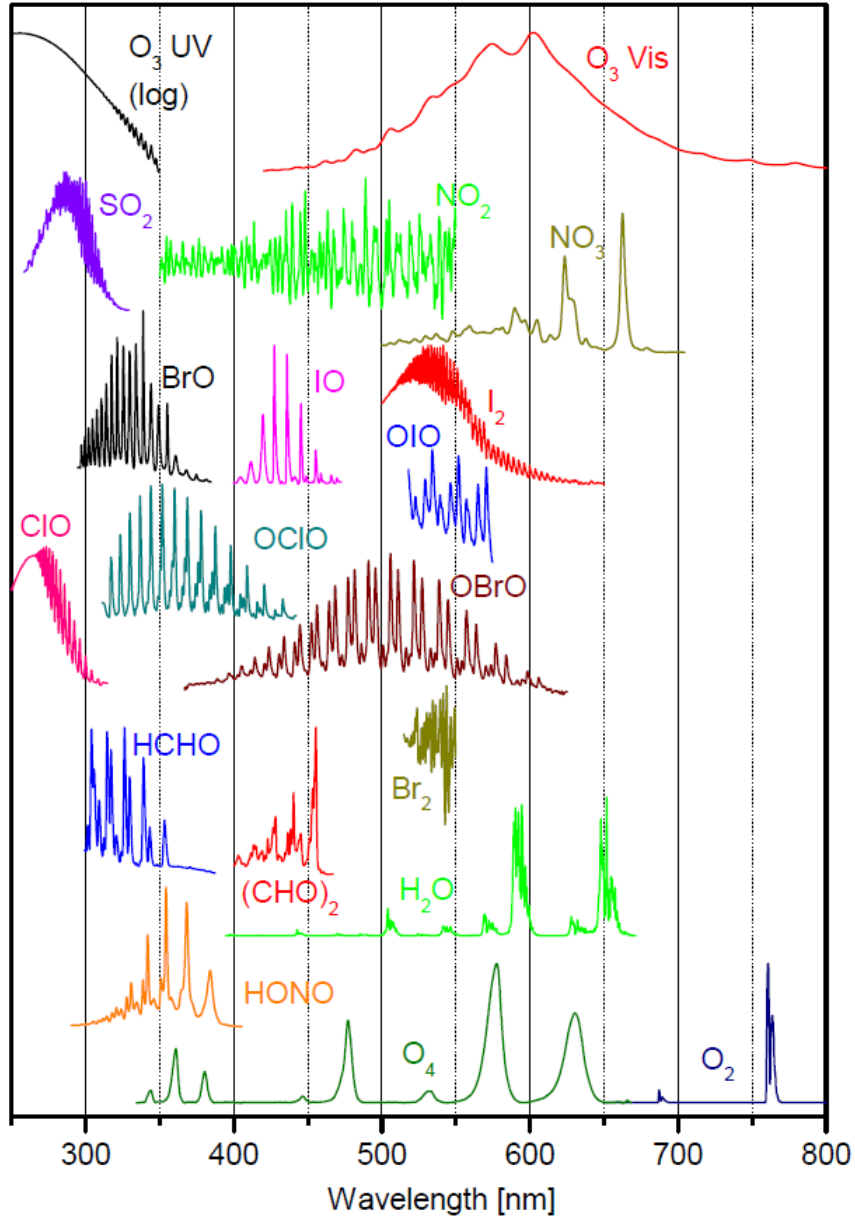
Figure 4.2: UV/Vis absorption cross sections of atmospheric trace gases detectable by DOAS.

lines, as wavelengths on either side of the line are shifted into it. The magnitude of the so-called Ring effect depends on the atmospheric path lengths of the photons entering the spectrometer. The longer the path in the lower atmosphere where the air density is higher, the more likely a Raman scattering event becomes. Therefore, the Ring effect is dependent e.g. on the solar zenith angle, the cloud cover and the aerosol concentration in the atmosphere. To correct for the Ring effect, a so-called Ring spectrum $R(\lambda)$ is calculated (e.g. by DOASIS, Figure 4.3).

4.2.2 Broadband Components

The light is affected by scattering and absorption on aerosol particles and cloud droplets (Mie scattering) and by scattering on air molecules (Rayleigh scattering) [1]. Both Mie scattering ε_M and Rayleigh scattering ε_R are elastic, i.e. the wavelength of the scattered photons remains

---

[1]More precisely, we mean the Cabannes line of Rayleigh scattering. In a strict nomenclature, Rayleigh scattering also includes rotational Raman lines (mentioned above), but these are treated separately in the DOAS approach because of their effect on narrowband spectral structures. For clarity, see [37].
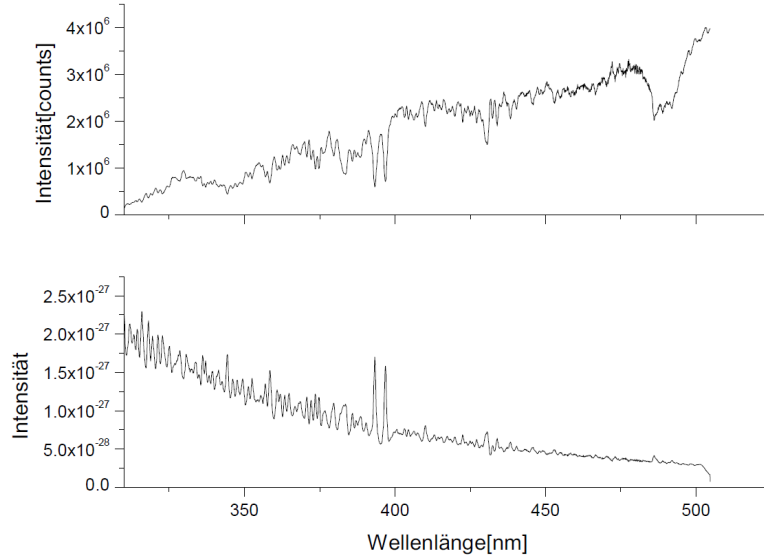
Figure 4.3: An example of a Fraunhofer spectrum (top) and the Ring spectrum calculated from it (bottom).

constant during the process and have their respective cross-sections. The Rayleigh scattering probability is proportional to λ^{-4}, so shorter wavelengths are more likely to be scattered than long wavelengths. This is the reason why the sky appears blue. Mie scattering is much less dependent on wavelength, so clouds and fog appear white, as all wavelengths are equally scattered.

For the sake of integrity it should be noted that some trace gas cross sections also have broadband parts $\sigma_{i0}(\lambda)$ in addition to the narrowband parts mentioned above.

4.2.3 Modified Lambert-Beer Law

Considering sections 4.2.1 and 4.2.2, we expand Equation 4.3:

$$I(\lambda, L) = I_0(\lambda) \cdot \exp\left(-R(\lambda) - \sum_i \sigma_i(\lambda) \cdot S_i(\lambda)\right) \cdot \tag{4.6}$$
$$\exp\left[-L \cdot \left(\sum_i (\sigma_{i0}(\lambda) \cdot \rho_i) + \varepsilon_R(\lambda) + \varepsilon_M(\lambda)\right)\right]$$

Here, the first exponent contains all narrowband components and the second exponent contains all broadband components.

4.2.4 The DOAS fit

Solving equation 4.6 for $\ln(I/I_0)$ yields the *optical density* τ:

$$\tau = \ln\left(\frac{I(\lambda)}{I_0(\lambda)}\right) \tag{4.7}$$
$$= -R(\lambda) - \sum_i \sigma_i(\lambda) \cdot S_i(\lambda) - \sum_k b_k \lambda^k$$

Here, $\sum b_k \lambda^k$ is a polynomial to account for the second exponent of equation 4.6, which includes all broad band features, as mentioned in section 4.2.2. $R(\lambda)$ is the Ring spectrum and $\sigma_i(\lambda)$
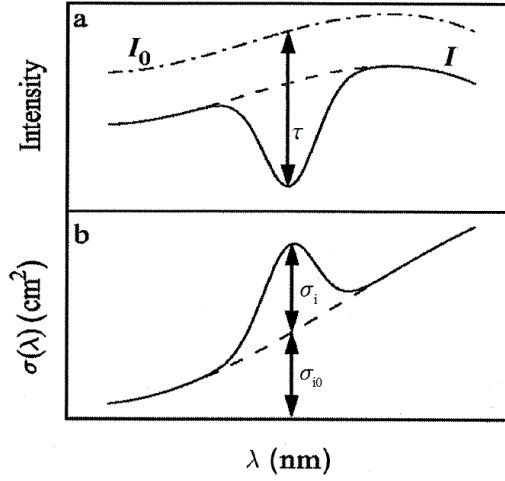
23

Figure 4.4: *The principle of DOAS: The optical density τ is the result of narrow σ_i and broadband parts σ_{i0} of an absorption cross section. Adapted from* [22].

and $S_i(\lambda)$ are the cross section and the slant column density of trace gas i, respectively. Apart from atmospheric effects, the instrument itself also modulates the signal: The signal from light reflected from elements in the spectrometer or the 0th or 2nd order of scattering from the grating are called *spectrometer stray light*. If stray light intensity varies over the spectrum, absorption bands at different wavelengths will be changed differently, i.e. the optical density will be reduced more for some parts of the spectrum than for others. In order to account for this, a so-called 'Offset' polynomial $I_{Ofs}(\lambda)$ can be added in the fitting procedure (see equation 4.8).

The idea of the DOAS fit is fairly simple. A model is used to construct an optical density by taking into account all the physical effects the light entering the instrument undergoes. This modelled optical density is then compared to the measured optical density. By varying the physical parameters of the model (which include the trace gas column densities S_i), the difference between model and measurement are minimized. When the minimum is reached, the physical parameters of the model are assumed to represent those of the measurement.

Due to noise in the measurement (see section 4.4.3), the modelled optical density can never perfectly match the measured optical density. Therefore, the DOAS fit searches for the minimum quadratic deviation (dependencies omitted for readability):

$$\chi^2 = \left[\ln\left(\frac{I_0 + I_{Ofs}}{I} \right) - R - \sum_i \sigma_i \cdot S_i - \sum_k b_k \lambda^k \right]^2 \tag{4.8}$$

The unexplained remainder of the spectrum after minimisation (by varying the parameters S_i and b_k) is called the fit residual. The smaller the residual, the better the fit has succeeded in modelling the trace gas absorption. Ideally, the residual is only composed of noise. In order to detect a trace gas, its optical density needs to be larger than the residual. This criteria can be used to estimate the detection limit for a particular species. Once the minimum was found, the fit parameters S_i represent the column densities of the individual trace gases.

4.3 Calculating trace gas concentrations

Depending on the measurement geometry, the column densities obtained with the evaluation described above need to be interpreted in different ways. One way is the assumption of simplified
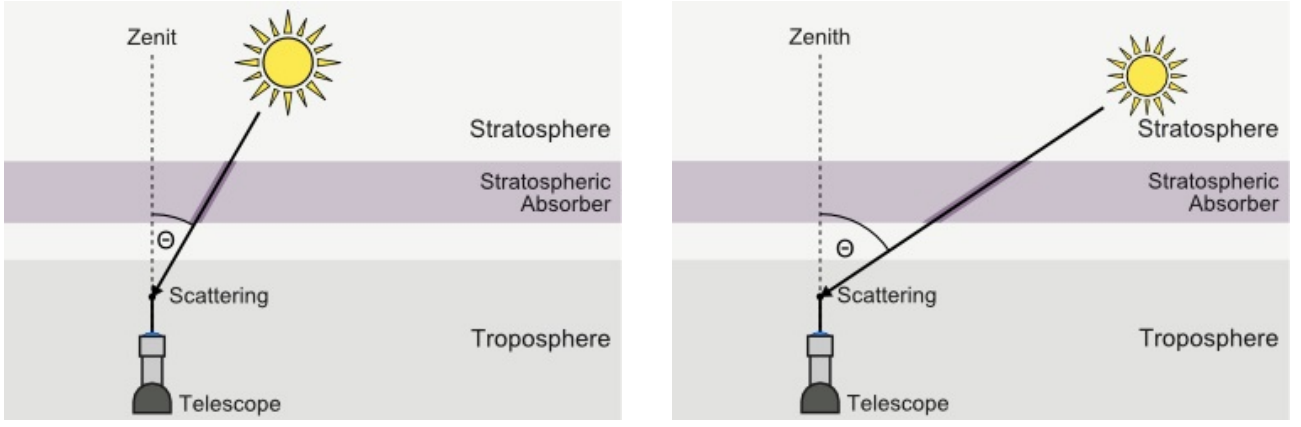
Figure 4.5: Light path through the atmosphere in the case of small (left) and large (right) solar zenith angle. With larger SZA, the light path through a stratospheric absorber is enhanced.

geometrical approaches (like in this experiment as described in the following sections), but in more complex cases, extensive radiative transfer simulations have to be carried out (section 4.3.4). The observation geometry can be described by the *solar zenith angle (SZA)* θ (angle between the zenith and the sun) and the *telescope elevation angle* α (angle between the horizon and the viewing direction). The light path also depends on the *solar relative azimuth angle (SRAA)*, which is neglected here.

4.3.1 Active measurements

Active measurements are measurements with an active or artificial light source. In modern applications, often LEDs are used because of their well defined spectra. For active measurements, the interpretation of the retrieved column densities is the simplest, because the light path is clearly defined. It runs from the light source to the DOAS instrument. Dividing the column density by the length of the light path directly yields the average trace gas concentration along the light path. There are some similar applications, where the instrument points directly at the sun or the moon (*direct light measurements*).

4.3.2 Zenith sky measurements

Zenith sky measurements are performed by looking straight up with a passive instrument. In this geometry, the exact light path is unclear, but radiative transfer models can be used to make a statistical prediction about the average path. In order to compare different SCDs (which depend on the light paths), one can calculate the *Vertical Column Density* (VCD or V) from the SCDs with the help of the so-called *Air Mass Factor* (AMF or A):

$$\text{AMF} = A(\theta) := \frac{S(\theta)}{V} \approx \frac{1}{\cos(\theta)} \tag{4.9}$$

This approximation for the case of zenith sky measurements (valid for $\theta < 75°$) is illustrated in figure 4.5. The Fraunhofer reference is typically taken at the minimal solar zenith angle around noon. Therefore, the retrieved column densities are all relative to this value. The total SCD is the sum of the ΔS and the column density already present in the Frauhofer spectrum S_F.

$$S = \Delta S + S_F \tag{4.10}$$

S_F can be extracted with the help of a *Langley Plot*.

Langley plot

In a so-called *Langley Plot*, the measured ΔSCD is plotted as a function of the air mass factor AMF. If the concentration of a measured trace gas is constant during the course of the day the correlation between the ΔSCD and the AMF will be linear:

$$V = \frac{S(\theta)}{A(\theta)} \qquad (4.11)$$

$$= \frac{\Delta S(\theta) + S_F}{A(\theta)}$$

$$\Rightarrow \Delta S\left(A\left(\theta\right)\right) = V \cdot A\left(\theta\right) - S_F \qquad (4.12)$$

Here, θ is the solar zenith angle. If a constant concentration is assumed, the resulting plot can be extrapolated to $A = 0$. Here, $\Delta S = -S_F$, and the column density in the Fraunhofer reference spectrum can be retrieved (see figure 4.6). Note that the assumption of a constant concentration is only valid for a few atmospheric absorbers, e.g. stratospheric ozone.
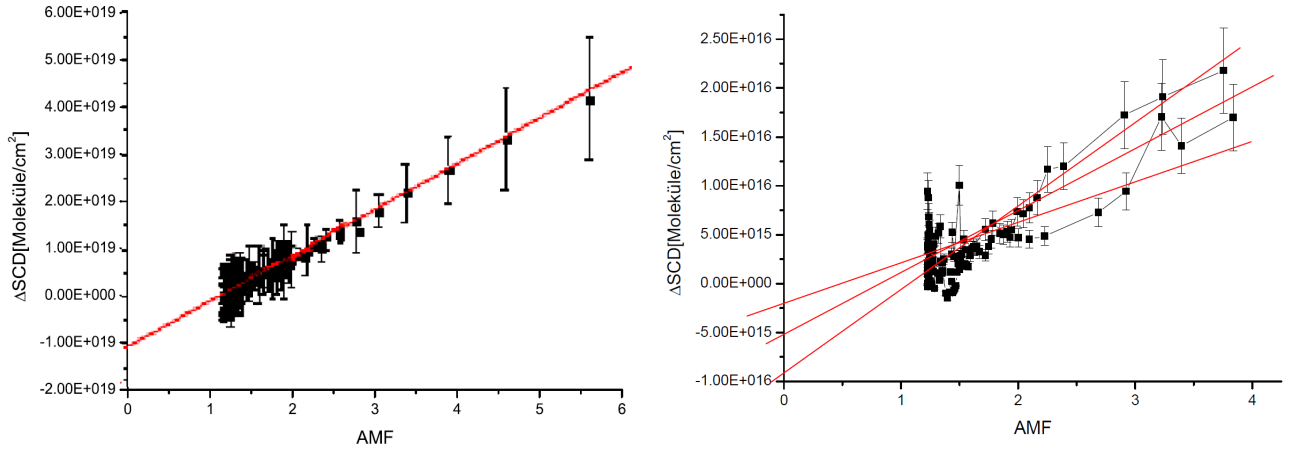

Figure 4.6: *Two examples of Langley Plots. The left panel depicts the Langley Plot of an ozone measurement. Extrapolation yields a Fraunhofer SCD of approximately 10^{19} molec/cm². The panel on the right is a Langley Plot of a nitrogen dioxide measurement. Here, the concentration is not constant during the course of the day, and the extrapolation does not yield a definite value.*

4.3.3 Multi-Axis-DOAS

The method of *multi-axis* DOAS (MAX-DOAS) strongly enhances the sensitivity for trace gases located in the troposphere (for details, see [13]). When observing light with small elevation angles α (angle between the horizon and the viewing direction of the instrument), the light paths through the lowermost atmospheric layers (and the SCDs of trace gases present there) are strongly enhanced, as shown in figure 4.7. However, the light path through the stratosphere does not change with elevation angle α. This offers the opportunity to distinguish between stratospheric and tropospheric trace gases. This usually means recording the Fraunhofer reference spectrum in the zenith direction to minimize the light path through the lower layers of the atmosphere. The airmass factor of a trace gas near the surface measured at an elevation angle α can be approximated by:

$$A(\alpha) \approx \frac{1}{\sin(\alpha)} \qquad (4.13)$$

However, light paths can become very complicated. For very small elevation angles, parts of the observed light are scattered within the trace gas layer. Multiple scattering can occur for high aerosol loads and under cloudy conditions. The geometric approximation (equation 4.13) is not valid anymore under these conditions. An example of MAX-DOAS measurements is shown in figure 4.8.
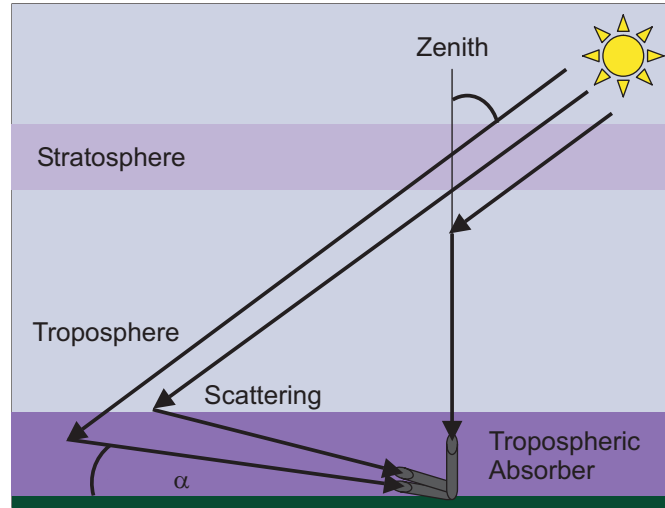

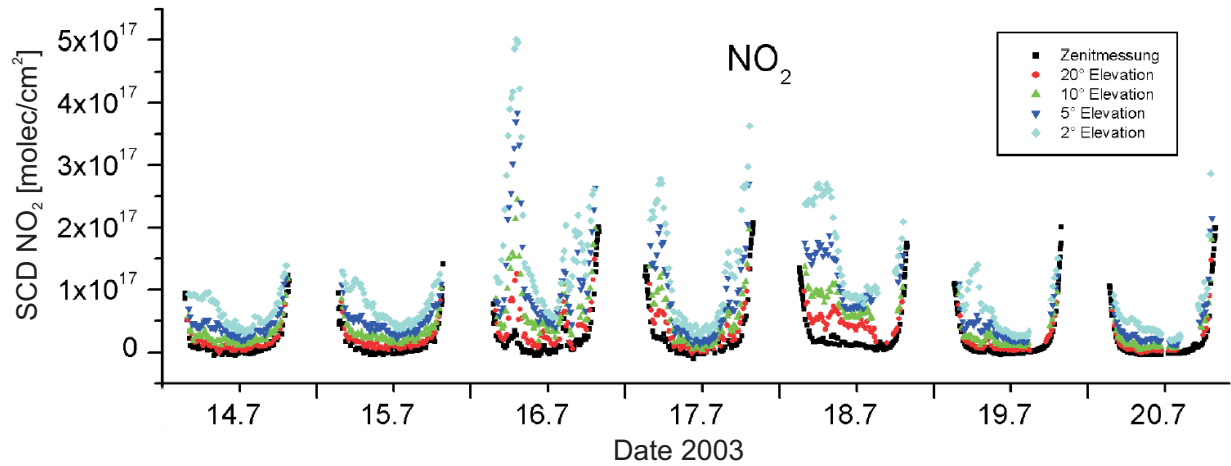Figure 4.7: *Observation geometry of MAX-DOAS measurements.*

Figure 4.8: *NO_2 SCDs measured with a MAX-DOAS instrument in Heidelberg. Different colours indicate different telescope elevation angles. The SCD increases with decreasing elevation angle, indicating the presence of NO_2 near the surface. The U-shape of the diurnal profile is caused by stratospheric NO_2.*

4.3.4 Complex scenarios

In case of heavy aerosol loads, clouds and more complex measurement geometries, such as from satellites, aircraft and ships, the approximations described above are no longer useful, because the light path distributions can become very complex. For example, figure 4.9 illustrates two basic cases for cloud influence on light paths. Light path distributions can be simulated by radiative transfer models (figure 4.10). A Levenberg-Marquardt algorithm [17, 18, 24, 25] then searches for minima in a χ^2 landscape to retrieve radiative transfer model parameters (e.g. aerosol load and trace gas concentrations) that best represent measured slant columns on the one hand and knowledge about the atmosphere on the other hand. Examples of this approach can be found in e.g. [8, 9, 14, 23, 33].
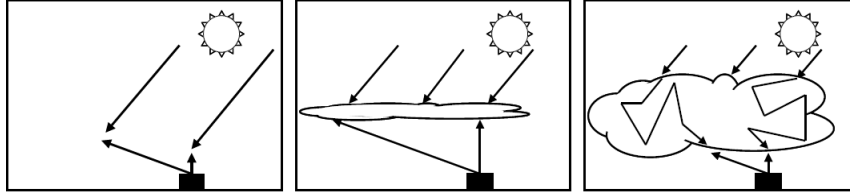

Figure 4.9: *Left: for clear sky, sun light is scattered by air molecules and aerosol particles towards the instrument. Center: diffusing screen effect: in the presence of thin clouds, a substantial fraction of the observed photons is scattered by the cloud; especially for the smaller elevation angles, this effect leads to an increase of the absorption path. Right: for optically thick and vertically extended clouds, multiple scattering can lead to a very large increase of the photon paths inside the clouds.* [34]
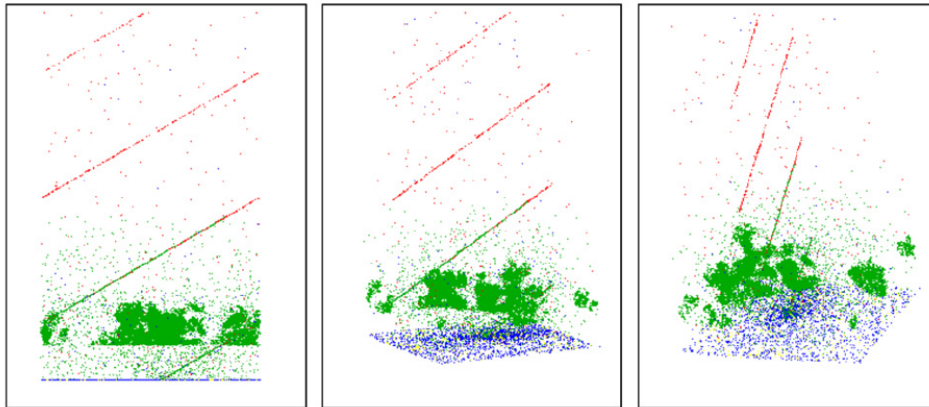
Figure 4.10: *Three different perspectives of events simulated by McArtim, a 3D backward trajectory monte-carlo radiative transfer model, when observing a cumulus cloud at 670 nm. Green points represent cloud and aerosol particle scatter events, blue points depict absorption events. Ground scattering is shown in yellow and red dots symbolize Rayleigh scattering by air molecules and hint to the lines of sight of the instrument.* [6]

4.4 Background and noise

The spectra are collected by grating spectrometers with CCD detectors. The properties especially of the detectors have to be taken into account in order to correctly record and process the spectra.

4.4.1 Electronic offset

The offset is an electronic signal (e.g. an analogue voltage or current) which is added to the photon induced signal of each pixel for every exposure, because the AD-converter can not convert a negative input. The offset can therefore best be measured by recording an exposure at a very low exposure time with no light entering the spectrometer, as the measured signal will then consist almost exclusively of the offset signal. To minimize the noise, however, it is best to record many such scans in succession. For the Ocean Optics USB2000, e.g., typically 10000 scans at 3 ms (minimum exposure time of this spectrometer) exposure time are recorded (figure 4.11, left panel). As the offset is added to each scan, the resulting spectrum must first be scaled to the measurement spectrum by the number of scans before it is subtracted:

$$I_{OS}(n) = I(n) - \frac{N_{Meas}}{N_{OS}} \cdot O(n) \tag{4.14}$$

Here, $I(n)$ is the intensity measured at each pixel n, $O(n)$ is the electronic offset, and N is the number of scans with which the respective spectra were recorded.
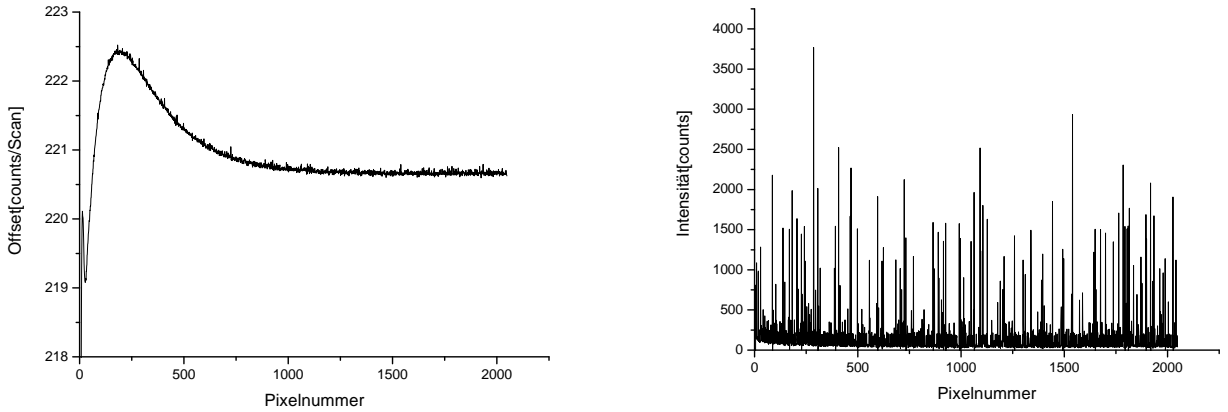

Figure 4.11: *Left: Offset spectrum recorded with an Ocean Optics USB2000 spectrometer. Most pixels have an average offset of about 221 counts/scan. For a typical measurement with saturation 75%, this is approximately 7% of the measured signal. Right: Dark current spectrum recorded at an exposure time of 60 seconds with a USB2000 spectrometer. Most pixels register a dark current of less than 4 counts per second, but a few so-called* hot pixels *register much more.*

4.4.2 Dark current

The dark current is caused by thermally excited electrons which pass the semiconductor band gap due to Boltzmann statistics. Therefore, it strongly depends on the temperature of the detector. In many spectrometers, the detectors are cooled to keep the dark current low. This is especially important for modern UV-sensitive back-thinned detectors, as the dark current is very high otherwise.

For a constant temperature, the dark current signal is proportional to the exposure time. To measure the dark current it is therefore best to use a long exposure time and only one exposure, so the offset is only added once. Of course no light should enter the spectrometer during the measurement. For the USB2000, the maximum exposure time is 60 seconds (figure 4.11, right panel). After the measurement is recorded, the offset must be corrected and the remaining signal is the dark current. When correcting for the dark current of a measurement

spectrum, the measured dark current must be scaled to the measurement exposure time before it is subtracted:

$$I_{DC}(n) = I(n) - \frac{t_{Meas}}{t_{DC}} \cdot D_{OS} \qquad (4.15)$$

Here, $I(n)$ is the intensity measured at each pixel n and D_{OS} is the measured dark current after correcting for the electronic offset. Before subtracting it, it is multiplied by the ratio of the measurement exposure time and the dark current exposure time.

4.4.3 Noise

Two spectra will never be perfectly identical, even if they are recorded under identical conditions. The reason for this is statistic noise in the photon signal and the detector background signal and additionally systematic noise. The statistic noise can be quantified. A measurement spectrum $I = I_B + I_P$ is always composed of the background I_B and the signal induced by the incident photons I_P. If multiple spectra are recorded under identical conditions, both contributions will fluctuate around a mean value. Gaussian error propagation yields the following equation for the total noise σ:

$$\sigma = \sqrt{\sigma_B^2 + \sigma_P^2} \qquad (4.16)$$

The background noise σ_B is a property of the instrument and is therefore often referred to as instrument noise. It is composed of fluctuations in the electronic offset and the dark current. The photon noise σ_P is a fundamental physical phenomenon. For a given light intensity, the number of photons in a certain time interval fluctuates. The number of registered photons is then distributed according to the Poisson distribution: If M photons are registered on average for a given time interval, the root mean square (RMS) of the obtained distribution will be $\sqrt{M}$. Spectroscopy instruments are designed so that the photon noise, not the instrument noise limits the instrument precision (see figures 4.12 and 4.13).

To measure both the instrument and the photon noise, two spectra I_1 and I_2 are recorded in quick succession, so the magnitude of the noise contributions in the two spectra can be assumed to be equal. If the two spectra are then subtracted from each other, the noise of the difference σ_D calculates to:

$$\sigma_D = \sqrt{\sigma_{I_1}^2 + \sigma_{I_2}^2} \qquad (4.17)$$

$$= \sqrt{2\sigma_I^2} \qquad (4.18)$$

$$\Rightarrow \sigma_{I_i} = \frac{1}{\sqrt{2}}\sigma_D \qquad (4.19)$$

Note that this is the *average* noise over all pixels. The instrument noise can vary 20-30 % from pixel to pixel in modern CCDs [27]. In order to be entirely precise one would therefore have to characterise the instrument noise of each pixel separately, but since under reasonable measurement conditions photon noise largely dominates the overall noise in a spectrum, it is not necessary to deal with this 'noise of the instrument noise'. When collecting more and more light, at a certain point all statistical noise is so small that only systematic noise remains in the residual.

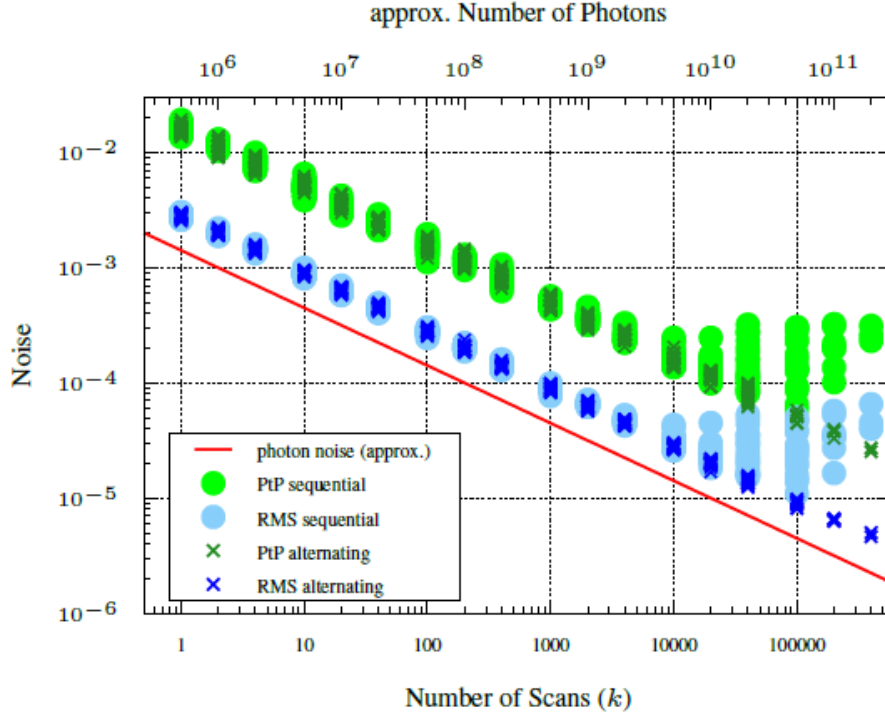Figure 4.12: *Noise measurements of a modern DOAS spectrometer. All statistical noise can theoretically be reduced indefinitely by adding up more photons (scans), but at a certain point systematic noise remains.* [10]
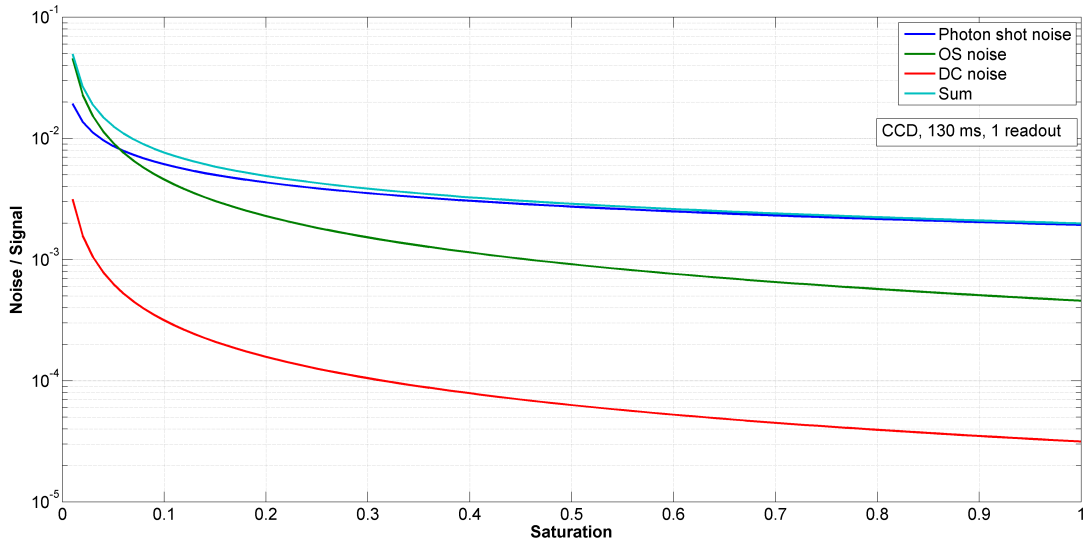

Figure 4.13: *Calculation of the statistical noise contributions in a single readout of a modern CCD for different saturations. Photon noise is the largest statistical noise source for saturations > 5 %.* [27]

4.5 Summary

Each measured spectrum is composed of several superimposed signals:

1. *Background.* The background signal is the measured signal when no light enters the spectrometer (section 4.4). It consists of:

   - *Electronic offset*: Proportional to the number of scans recorded.
   - *Dark current*: Proportional to the exposure time.

2. *Narrowband effects* (section 4.2.1)

   - *Fraunhofer spectrum*: The Fraunhofer spectrum is the spectrum of the sun as it arrives at the top of the earth's atmosphere. It already contains many very strong absorption structures. These are caused by light absorption by species in the sun's outer layers (photosphere).
   - *Trace gas absorption*: Trace gases in the atmosphere create characteristic absorption structures in the measured spectra. The goal of the DOAS retrieval is to identify and isolate these structures, which typically feature optical densities between 10^{-3} and 10^{-1}.
   - *Raman scattering*: Inelastic scattering filling in Fraunhofer lines.

3. *Broadband effects* (section 4.2.2)

   - *Broadband absorption cross sections*
   - *Rayleigh & Mie scattering*: Elastic scattering either by air molecules (Cabannes line of Rayleigh scattering) or by small water droplets or particles called *aerosols* (Mie scattering).
   - *Spectrometer stray light* (section 4.2.4)

4. *Noise* (section 4.4.3)

   - *Instrument noise*: The dark current signal follows a Poisson statistic and its noise is therefore proportional to the square root of the dark current signal. The offset noise is proportional to the square root of the number of scans. Therefore, the instrument noise (made up of offset and dark current noise) is also proportional to the square root of the number of scans.
   - *Photon noise*: The photon signal follows a Poisson statistic. Its noise (shot noise) is therefore proportional to the square root of the signal.
   - *Systematic noise*: Sources for systematic noise can be unexplained physical changes in the instrument or in the atmosphere. *Can you think of some sources of systematic noise in this experiment?*

The optical density τ calculated from two spectra I and I_0 is then fitted with the least squares method according to equation 4.8. The resulting slant columns S can be converted to vertical columns and concentrations with knowledge about the light path, see section 4.3.

Chapter 5

Experimental setup

This experiment is conducted at the Institut f r Umweltphysik (INF 229), Room 238. During the course of the measurements, the spectra of scattered sunlight as well as those of some artificial light sources will be examined. In both cases, a telescope is used to collect the light. For the atmospheric measurements, a telescope mounted on the roof of the building is used (see figure 5.1). For the laboratory studies, another telescope mounted on an optical bench is employed (figure 5.2).

5.1   General setup

The respective telescope is connected to the spectrometer with a 400 μm diameter quartz fibre bundle with a numerical aperture of 0.22 and protected by a metal tube. The quartz fibre is easily damaged, so please handle it with care. The fibres of the spectrometers can either be connected to the roof telescope fibres or to the lab telescope by couplings.

The spectrometers are located in a metal housing. This housing contains thermoelectric cooling units which are used to stabilize the spectrometer temperature. The data recorded by the spectrometer is sent to a PC via the USB interface. Figure 5.2 gives an impression of the instrumentation.

5.2   The spectrometer

The commercial miniature spectrograph-detector unit Ocean Optics USB2000 represents the heart of the DOAS instrument. It is built in the *Czerny-Turner* design (see Figure 5.3). The light entering the spectrometer through a slit is collimated by a spherical mirror and projected on a grating as a parallel light beam. The grating disperses the light into its spectral components. A second spherical mirror focuses the light on a detector, which consists of a one-dimensional CCD array with 2048 pixels.

The most important features of the detector are:

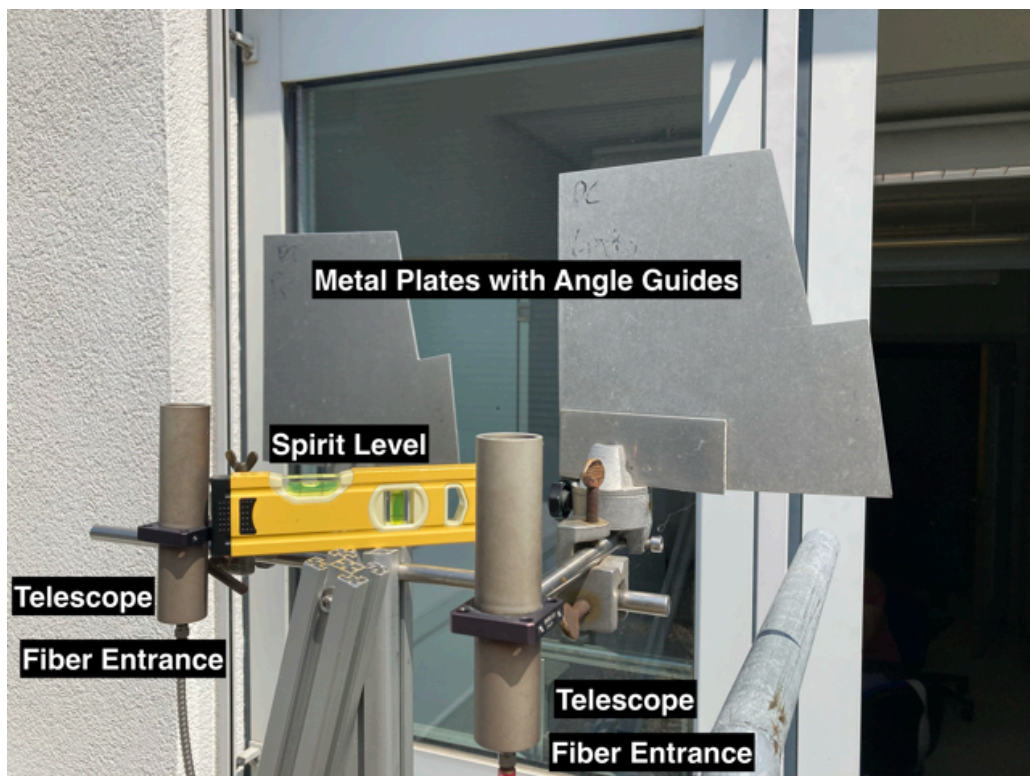| Number of pixels:	2048
Pixel size:	$14\mu m \times 200\mu m$
Full Well Capacity per pixel:	100 000 electrons
A/D - Converter:	12 Bit (i.e., 4096 Counts/Pixel)
Integration time:	3 ms - 65 s

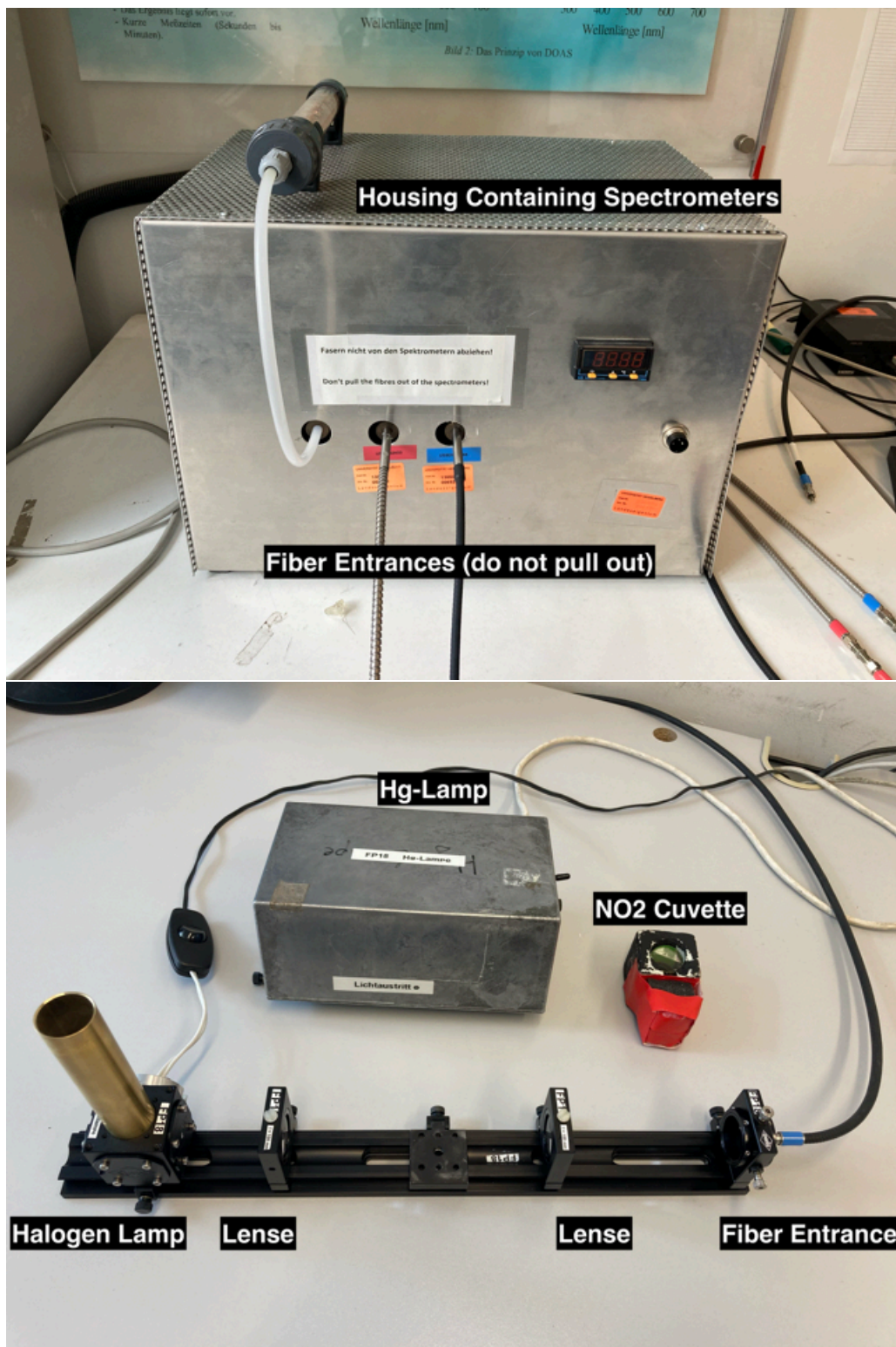Figure 5.1: *Telescopes to collect scattered sky light.*
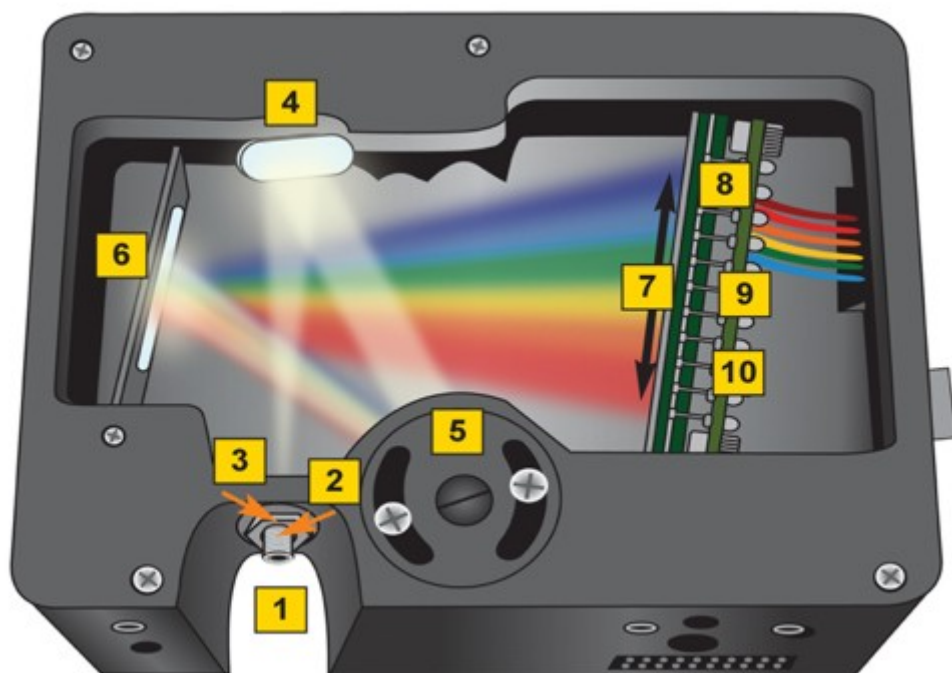
Figure 5.2: *Laboratory instrumentation.*

Figure 5.3: *The USB2000 spectrograph with detector. 1: fibre connector; 2: entrance slit; 3: optical filter; 4: collimating mirror; 5: grating; 6: focusing mirror; 7: collection lens; 8: CCD detector.*

Chapter 6

Software

This chapter describes which software is to be used to complete the experiment. The computer in use runs on a Windows 10 environment for evaluation and internet access, while the measurement system is a Windows XP virtual machine. This is required for the software DOASIS.

6.1 DOASIS

During this experiment, you will use the DOASIS (DOAS Intelligent System) software, which was developed at the Institut f r Umweltphysik in the scope of a PhD. DOASIS can be used to acquire data from the spectrometer and display it in a graphic user interface for evaluation. The program is written for Microsoft Windows, uses a typical Windows interface, and should therefore be easy to learn. When conducting measurements and performing data evaluations 'by hand', all functions are accessed via the menus at the top of the window. However, all functions can also be called from jscript programs. These scripts allow the automation of data acquisition and evaluations.

The DOASIS user interface is split into 4 areas, as shown in figure 6.1.

- *Spectrum Sheet*: This area is used for viewing the spectra. You can switch between all open spectra by clicking on the tabs at the top of the spectrum sheet. The y axis is automatically scaled to fit the displayed spectra. You can zoom in to any part of the spectra by holding the left mouse button down and dragging the mouse.

- *SpecBar*: You can use the Specbar to switch between open spectra. Alternatively, this window can be used to control the spectrometer by clicking on the *PDA* tab.

- *Information window*: This area gives you information on the current spectrum. You can switch between *Statistics* such as maximum, minimum, average and standard deviation (called *Deviation*) and *Properties* such as exposure time and number of exposures.

- *Console*: The console can display different things, depending on which tab you select:

  1. *Output* gives you information about called functions or running scripts.
  2. *Script* is used to start, stop and edit scripts.
  3. *Mini Scripts* can be used to quickly implement small scripts.
  4. *Quickscript* allows the user to define shortcuts to certain scripts.
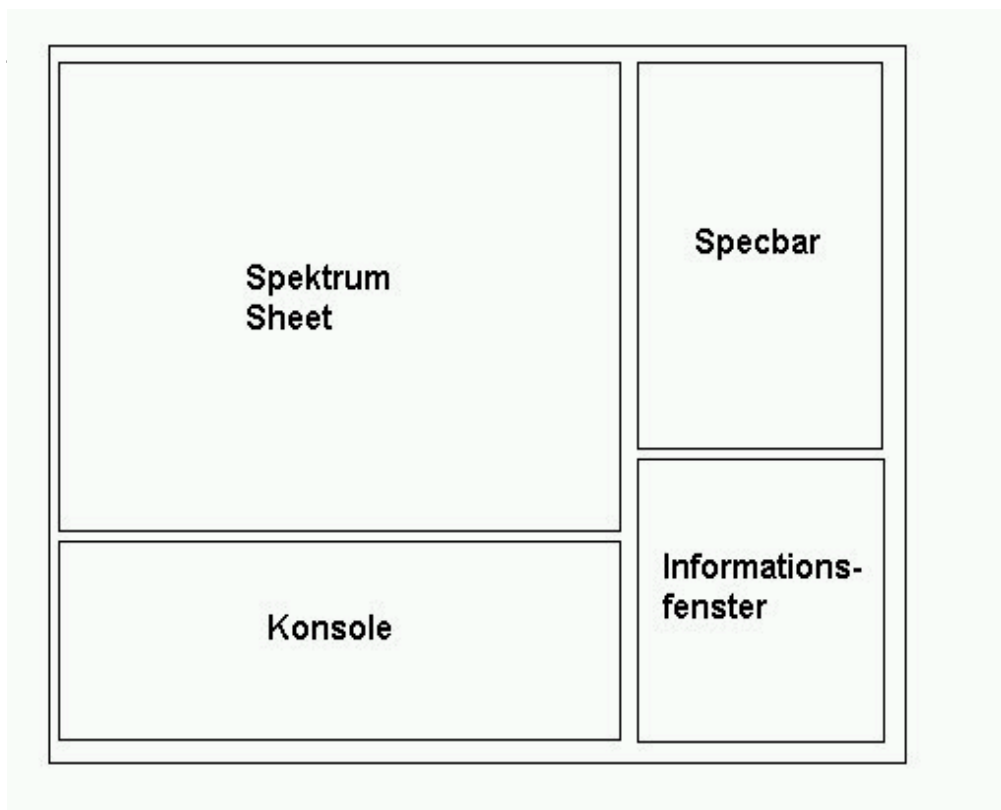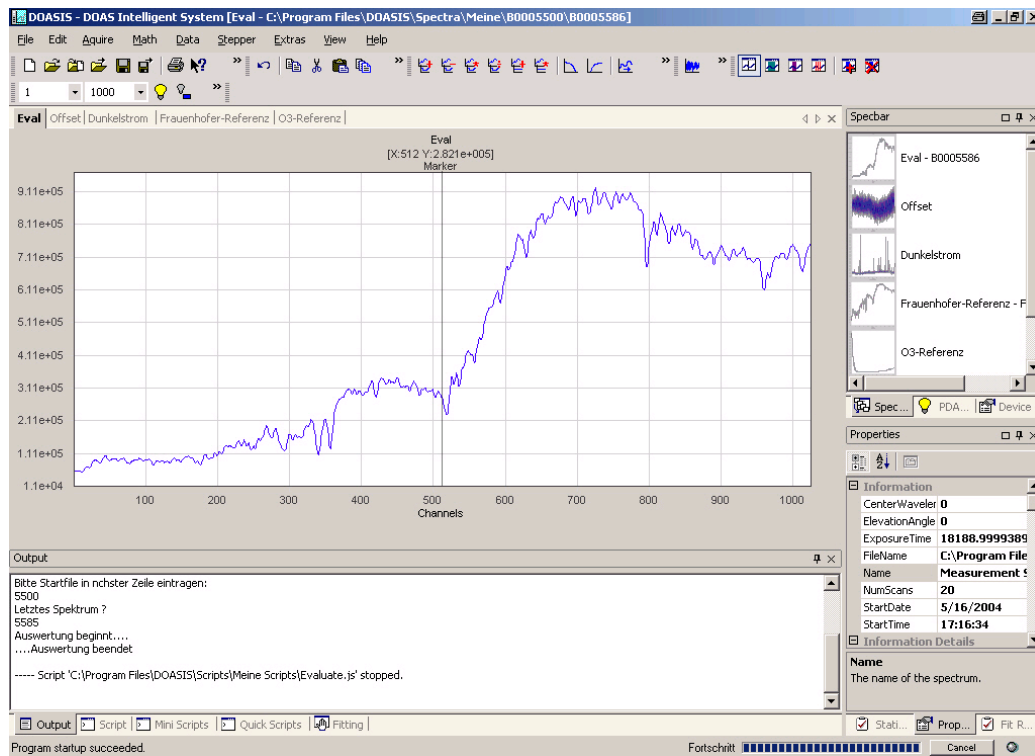 5. *Fitting* is used to run DOAS retrievals.

Figure 6.1: *The graphic user interface of DOASIS is split into 4 areas.*

First steps

1. Record a scattered light spectrum.
   To do so, change from the *Specbar* register to *PDA*. Set the *Device* to *Ocean Optics USB 2000*, if this has not been done yet. Below, you can set the spectrometer's exposure time in milliseconds and the amount of exposures to record (*NumScans*), see figure 6.2. Start the measurement by clicking on the *Scan* button.

2. Check the information DOASIS gives you.
   In the *Information* window under the register *Statistics* you will be given statistical information about the current spectrum such as the average number of counts (*Average*), the standard deviation from this value (*Deviation*) and the maximum number of counts (*Max*). Also take a look at the *Properties* register.

   The statistical information in the *Statistics* tab is calculated over the range selected with the Math marker (green). The Math marker can be toggled in the toolbar of DOASIS at the very top. There is also a regular Marker (black line), which shows the currently marked channel and (if the instrument has a calibration) the currently marked wavelength. Another important marker is the Fit Marker (red). When performing a DOAS fit, the range of the fit is determined by this Fit Marker, and values outside of it are not considered during this fit. The size of the the Math Marker and Fit Marker can be changed by dragging the left and right edges at the bottom of the screen.
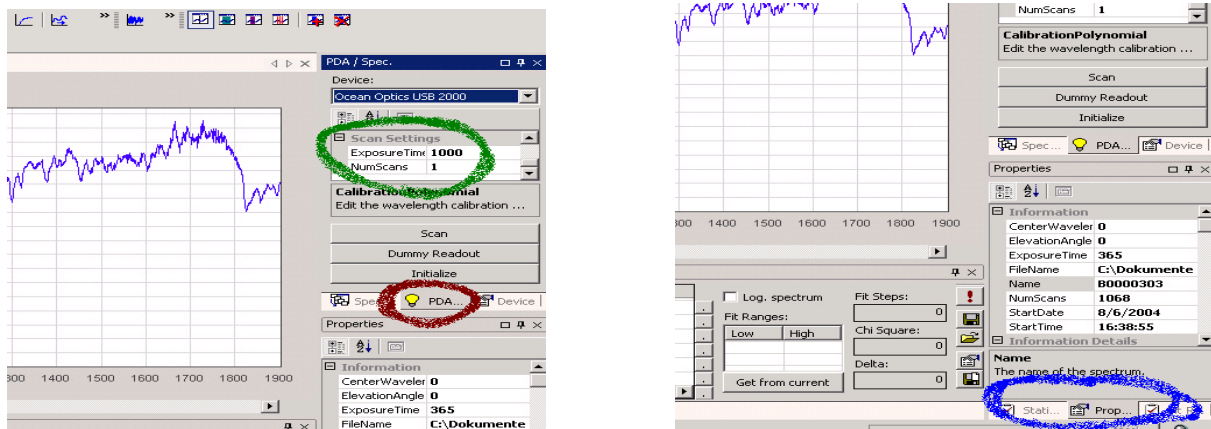
Figure 6.2: *Left side: In the PDA Register you can set the exposure time and number of exposures. Right side: The Properties register contains useful information about the current spectrum.*

3. Record further spectra.
   In order not to overwrite your first spectrum, use the menu command *File → New...* to open a new *Spectrum Sheet*. Play around with the exposure time and the number of exposures. Record an oversaturated spectrum. (Each pixel has a single exposure full well capacity of $2^{12} - 1 = 4095$ Counts.

4. Compare two spectra with each other.
   Use the menu command *View → Add Overlay...* to view two spectra on top of each other. If you use the option *Fit all overlays*, the y axis of the overlay spectrum will be adapted so that both spectra are fully visible on the screen.

5. Zoom in to an area of the spectrum.
Hold the left mouse button down while drawing a rectangle around the area of interest. The program will then zoom in to this area. Notice that the *Statistics* in the lower right corner of the screen also change. They now give information about the zoomed in region of the spectrum. Click the right mouse button on the *Spectrum Sheet* to zoom back out. Note, that the zoom rectangle should be drawn from left to right. Dragging from right to left occasionally causes errors.

6. Save your spectrum.
First, create your own folder in the directory

$$FPDaten\backslash FP\backslash FP - Praktikanten\backslash$$

and save all your files into this folder (except for special cases, which are noted in this script). **If you save your files somewhere else, they will be deleted.**
Open the save dialogue using *File → Save As...*. DOASIS supports a number of file formats. The standard format is **.sp2*. In this format, all spectrum properties are saved, and this is the format you should use during the experiment. The save dialogue also gives you the option to save the spectrum as a *.txt file. This can be useful if you want to, for example, plot some spectra with Python.

Troubleshooting DOASIS

Task Manager

- The Task Manager of Windows XP inside the virtual machine may be accessed using the key combination Ctrl + Shift + Esc.

DOASIS is crashing or freezing:

- Close DOASIS (you may need to use the Task Manager)

- Unplug the USB cable that connects the spectrometer to the computer. Plug it back in after waiting a few seconds.

- Restart DOASIS

Cannot stop automated scripts or scan in DOASIS:

- The scripts cannot be halted. Use the Task Manager to kill DOASIS.

Accidentally closed important tabs in the UI:

- You can restore the default settings for the DOASIS UI by going to View - Docking Windows - Reset Workspace Layout.

Chapter 7

Course Instructions

Please do NOT change the computer's time!

The quartz fibre is very sensitive! Do not forcefully bend it or it will break!
The computer should be switched on and automatically record spectra. Stop the automated measurements by clicking on the *Script* register on the bottom left corner of the screen, then click on the *Stop* button. The program will finish the current measurement, which may take a few minutes. If the window *Terminate Script* pops up, click *No*.
When you have familiarized yourself with the experimental setup and evaluation software, you can begin the experimental part of the course. The first measurements will take place in the lab room. Therefore, **CAREFULLY** unlock the fibre coupling. Do not touch the end of the fibre (because of fat and liquid on your skin). In order to record dark spectra, use a tissue, towel or something similar instead.
You should take screenshots of important spectra (DC spectrum, offset spectrum, Hg spectrum) and your DOAS fits, as the spectrum files can only be opened with the DOASIS software.

7.1 Characterizing the instrumentation

When recording a spectrum, two parameters must be taken into account: the *exposure time* and the number of exposures, also called scans. The exposure time is usually given in milliseconds and represents the time the detector is exposed to incoming light. The number of scans (called *NumScans* in DOASIS) tells the spectrometer how many exposures to add for each measurement.
It is important to use the dynamic range of the instrument's detector (see figure 4.13). If the exposure time is chosen too short, the recorded spectrum will consist almost exclusively of electronic offset and the noise pattern will be large. On the other hand, if the exposure time is too long, the detector will be oversaturated and the top of the spectrum will be cut off. *Why should either situation be avoided?*

The *saturation* T of a detector pixel P is defined as:

$$T(P) = \frac{C(P)}{N \cdot C_{max}} \cdot 100 \tag{7.1}$$

Here, $C(P)$ is the number of counts registered in the pixel, N is the number of scans. $C_{max} = 4096$ is the maximum number of counts the pixel can register. At saturations above 80%, the sensitivity of the CCD detector begins to drop off. Therefore, the measured signal is no longer proportional to the incoming photons. To avoid this, a saturation of about 70% is typically used for atmospheric measurements.

In this section you will learn about the composition of a measured spectrum and how to optimize your measurements. The spectrometer's detector is of special importance in this respect.

7.1.1 Offset

1. Record an offset spectrum.
   Cover the fibre so no light enters the spectrometer and record an offset spectrum. You should use at least 10,000 exposures at the minimal exposure time. Save the spectrum in the *.sp2 format and take a screenshot of it.

   Determine the mean offset value per pixel per scan. Use the Statistics *tab and if necessary the menu entry Math → Scalar Operations → . . .*

7.1.2 Dark current

1. Record a dark current spectrum.
   Use the maximum exposure time of 60 seconds. One exposure is enough here. Save the spectrum in the *.sp2 format and take a screenshot of it.

   Do you need to correct for the offset here? If so, use the menu entry Math → Correct Offset [1] *and then save the spectrum again. Determine the average number of counts per pixel per second caused by dark current and compare this value to the offset. Discuss the relevance of the dark current correction.*

2. Record at least 5 further dark current spectra at smaller exposure times.

   Is the dark current constant? Plot the average dark current signal against the exposure time.

When correcting your measurements for offset and dark current, the *Correct Offset* and *Correct Dark Current* functions in DOASIS will automatically deal with the calculations from chapter 4.4.1 and 4.4.2, which means you do not need to worry about the relative number of scans or exposure time of your offset/dark current spectrum and the measurement you want to correct.

7.1.3 Determining the instrument noise and total noise

Instrument noise

1. Take 2 offset spectra (10,000 exposures) back to back and calculate the difference (*Math → Spectrum Operations → Subtract Spectrum*). Determine the standard deviation (see *Statistics, Deviation*).
   Take a screenshot of the difference spectrum.
   How can the instrument noise of a single spectrum now be calculated?

2. Determine the noise for smaller exposure numbers.
   Use at least 5 sets of 2 spectra that were recorded under identical conditions, and do the

---

[1] The commands 'Correct Offset' and 'Correct Dark Current' automatically correct for different exposure times and number of exposures, so you do not need to do this by hand. However, it is important that the *Properties NumScans and ExposureTime* of the offset and dark current spectra are correct when these are saved.
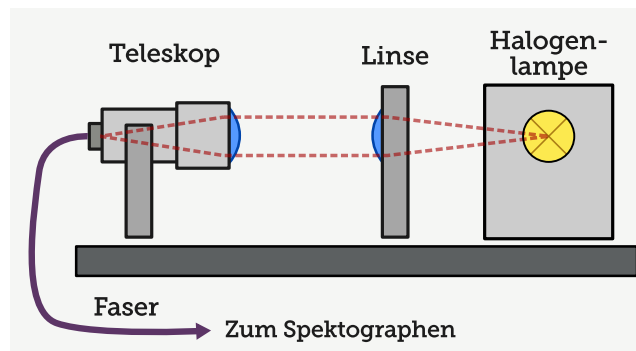
Figure 7.1: *Instrument setup for recording halogen lamp spectra.*

above calculation.
How should the instrument noise depend on the number of exposures? Plot the instrument noise against the number of exposures.

Total noise

1. Connect the fibre to the small optical bench for measuring light from the halogen lamp. Maximize the light throughput into the fibre by adjusting the lenses on the bench until you reach a saturation of about 60% for a small exposure time (< 100 ms).

   What is the optimal setup of the optical components? Hint: The light should be parallel between the two lenses.

2. Like with the offset spectra, record 5 sets of 2 halogen lamp spectra each to determine how the total noise depends on the number of exposures. Save all ten spectra.
   Correct both spectra for offset and dark current (*Math → Correct Offset . . ., and Correct Dark Current . . .*).

3. Take the difference of the two spectra of each set. Determine the standard deviation. This gives you the absolute total noise. If the lamp intensity drifted between the two evaluated measurements, systematic structures (typically of the shape of the lamp spectrum) will appear in your noise spectrum. In this case, a high pass filter has to be applied: For this purpose create a copy of the noise spectrum (*Edit → Duplicate*) and apply a low pass filter (*Math → Filter → Low Pass Binomial*, 1000 iterations). Subtract this low pass filtered spectrum from your original noise spectrum. Now, most systematic structures should be gone.

   If you see systematic structures in the spectrum that can not be explained by noise, consider adjusting the Math Marker to investigate only a certain range. What are the implications of doing this?

   Compare the total noise and the instrument noise.

4. Analogous to 3., take the quotient of the two spectra of each set. Then, take the logarithm of the quotient. This will give you the optical density of the relative total noise. Equivalent to the previous analysis, you may perform a high pass filter if you see systematic structures. Expressing the total noise in this form is useful in the context of DOAS,
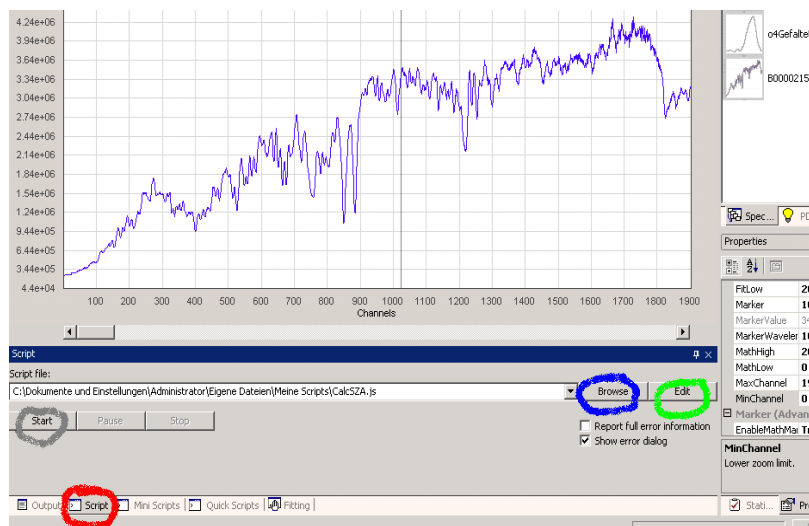
Figure 7.2: *The Script tab. Press the button* Browse *to open a script. The* Edit *button opens the script in a text editor. Press* Start *to start the script.*

as DOAS works with optical densities.

What do you expect the average value to be? Describe the dependence of the relative total noise on the saturation level and on the number of exposures. What is the physical explanation of the dependencies? Discuss the influence of the noise on the quality of atmospheric measurements.

7.1.4 Calibrating the spectrometer

1. Place the mercury vapour lamp on the optical bench for stability. Record a spectrum of the lamp at a good level of saturation (do not oversaturate the peaks!).

2. Correct for offset and dark current.
   You can use a script to save some time. Click on the script tab (see figure 7.2) and select the script *Offset&DunkelstromKorr.js*. Open it in the editor and check the paths in the script. They should be set to *FPDaten: \\FP \\Aktuell \\Korrekturspektren \\Offset.sp2 and FPDaten: \\FP \\Aktuell \\Korrekturspektren \\Dunkelstrom.sp2*. Please do not change the script. Instead, save the offset and dark current spectra you measured over the old ones at this location. Use the *Quick Scripts* tab next to the *Script* tab to link the script *Offset&DunkelstromKorr.js* to the hotkey position F2. Whenever you want to correct offset and dark current, you can now do so by simply pressing F2. This will start the script.

   From now on, all measured spectra must be corrected for offset and dark current! Nonetheless, you should also save an uncorrected version of every spectrum right after you take it.

3. Determine the Full Width at Half Maximum (FWHM) of the 4 largest mercury peaks by hand. The FWHM gives the optical resolution of the spectrometer.

What is the optical resolution of the spectrometer? Is it constant for all wavelengths?

4. Determine the wavelength calibration.
   Zoom in to a mercury peak and place the marker on the center of it (*View → Markers → show Marker*). You may also derive the center with a gauss fit on the line. The *Properties* window now gives you the channel number of the marker. Use figure 7.3 and the *Data Calibration Assistant* (*Data → Calibration Assistant*) to perform the calibration. Use a 2nd order polynomial. *Why shouldn't you use the peak at 313nm for the calibration?* When the calibration assistant finally asks, where the calibration polynomialshould be applied, set ticks at all the available options. Write down the polynomial coefficients as they appear in the *Output* window. From now on, your calibration will automatically be applied to all recorded and generated spectra. To still have the opportunity to manually recalibrate a spectrum, open the script *Kalibrieren.js* for editing and replace the old calibration coefficients with your new ones. Save the script and link it to the F3 key. You can now add the wavelength information to any measured spectrum by pressing F3.
   Note: The wavelength information displayed above the spectrum is not always accurate. To get the accurate wavelength of a certain pixel, double-click in the spectrum to move the Marker there and then click and hold the Marker. The accurate wavelength will be displayed at the upper end of the Marker, if you move the Marker around.

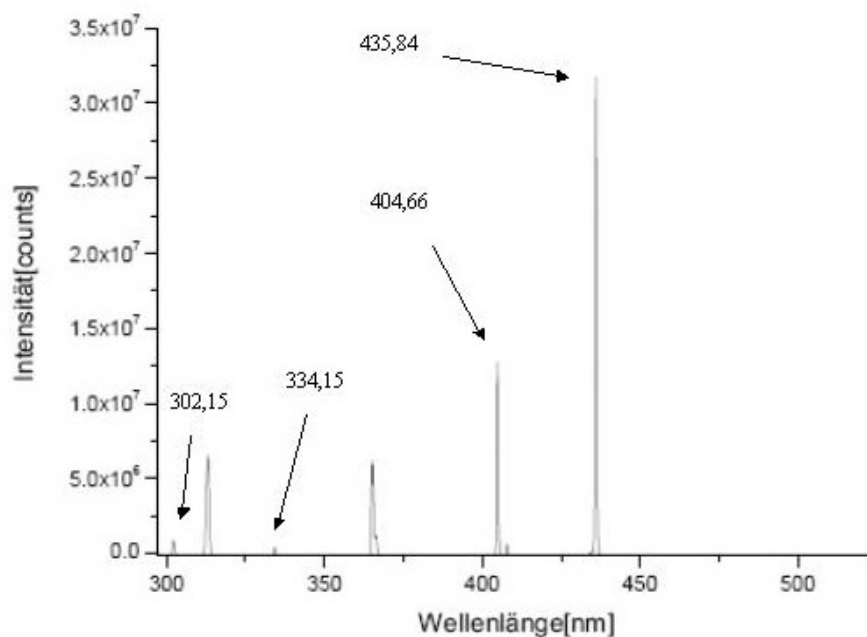*Determine the optical resolution of the spectrometer in nanometers.*

Figure 7.3: *Spectrum of the mercury vapour lamp recorded with the USB2000 spectrometer.*

7.2 Laboratory Measurements

In this part of the course, you will prepare a reference cross section of NO_2 and measure the concentration of NO_2 in a gas cell. You will learn how to run a DOAS fit.

7.2.1 Convolution of reference cross sections

The reference cross sections of the trace gases can be measured in the laboratory under controlled conditions, and many research groups are specialized on such experiments.[2] However, because these reference measurements are typically measured at a much higher wavelength resolution than used in the DOAS measurements, the references must first be adapted to the resolution of the spectrometer used in this experiment. This is done by convolving the high resolution reference cross-section with the DOAS instrument slit function. The slit function is the signal measured by the spectrometer when a monochromatic light source is observed and is a measure for the optical wavelength resolution of the instrument. The convolution smooths the reference and removes high resolution structures that the DOAS instrument cannot detect with its limited resolution.

The literature cross section is in units of $[\text{cm}^2]$, and represents the absorption of NO_2 as a function of the wavelength. It was recorded at a much higher resolution than our spectrometer has. In order to use this high resolution cross section in a DOAS evaluation of our spectra, it first needs to be smoothed to the resolution of our spectrometer. This is done by *convolving* it with the instrument point spread function. This function gives the optical resolution: it represents the spectral line shape of monochromatic light when measured by a particular spectrometer. In order to conduct this convolution, however, we first need to know the pixel - wavelength calibration of the spectrometer.

What is the convolution doing mathematically?

1. Zoom in to the single mercury vapour line at 404 nm. Place the green *Math Marker* (*View → Markers*) over the line. To move the *Math Marker*, move the mouse to the lower rim of the spectrum. An arrow will appear, which allows you to move the marker. Moving the mouse to the sides of the green area will allow you to resize it. Mark the mercury line so it is completely covered by the green area.

2. Place the *Marker* in the center of the mercury line, so that the area under the emission line on both sides of the vertical black marker is the same.

3. Create a new *Spectrum Sheet*(*File→ New...*) with 2048 channels. This sheet will contain the result of the convolution. **It needs the spectrometer's wavelength calibration (F3)!**

4. Open an NO_2 literature cross section spectrum.
   You will find literature cross sections in the folder *Referenzspektren.*

5. With NO₂ opened in the spectrum sheet, select *Math → Convolute....* The *Convolution Kernel* is your mercury line. The Target is the new spectrum you just created which has your wavelength calibration. Don't use *Auto search peak in kernel*, but do use *Normalize convolution kernel.*

6. At this point, call your experiment adviser to check that all settings are done correctly. This may save you a lot of time.

7. Run the convolution. *Compare the high resolution reference cross section with the convoluted cross section. How do they differ?*

8. Save the convolved absorption cross section. I recommend a simple name like *no2conv, o3conv, ...*

---

[2]A comprehensive database of relevant atmospheric species can be found at http://www.uv-vis-spectral-atlas-mainz.org/

9. Repeat the above steps to convolute references for ozone, O_4 and H_2O. You will need these references for the evaluation of the atmospheric measurements.
   What is the effect of the convolution on these references?

7.2.2 Recording a spectrum of the NO_2 gas cell

We will now hold a gas cell of length L into the light path between the halogen lamp and the fiber. The Lambert-Beer equation 4.3 can then be written in a simplified form:

$$I(\lambda, L) = I_0(\lambda) \cdot \exp(-\sigma_{NO_2}(\lambda) \cdot \rho_{NO_2} \cdot L) \tag{7.2}$$

$I(\lambda)$ and $I_0(\lambda)$ can be measured directly in this experiment.

1. Record and save a well saturated spectrum of the halogen lamp without any gas cells between the lamp and the fiber. How many exposures are required? Remember that you want to evaluate for NO_2, so make sure the saturation level of the spectrum is good in the wavelength range you later want to do the evaluation in. Some parts of the spectrum may be oversaturated ...

2. Repeat the measurement, but this time place the gas cell between the lamp and the fiber. Save your spectrum.

Using the 2 spectra you just recorded, you now can calculate the concentration of NO_2 in the gas cell. To do this, you will need the convoluted reference cross section of NO_2 you prepared in the previous section.

7.2.3 Determining the NO_2 concentration in the gas cell

By directly applying the Beer - Lambert law of absorption, you can now calculate the NO_2 concentration.

1. Correct your measured spectra for offset and dark current.

2. Divide the spectra by each other (*Math → Spectrum Operations→ ...*).

3. Take the logarithm (*Math → Logarithm*).

By performing the above steps, you have calculated the optical density τ from equation 4.7:

$$\tau = \ln\left(\frac{I_0(\lambda)}{I(\lambda)}\right) = \sigma_{NO_2}(\lambda) \cdot \rho_{NO_2} \cdot L \tag{7.3}$$

Why is it unproblematic if the saturation or the number of scans of the two spectra is different?

σ_{NO_2} is the cross section of NO_2, which you have prepared for this spectrometer. In order to calculate the concentration ρ_{NO_2}, we will now perform a least-squares fit. This fit varies the SCD such that χ^2 in the following term is minimized (compare equation 4.8):

$$\chi^2 = \left[\ln\left(\frac{I_0(\lambda)}{I(\lambda)}\right) - S_{NO_2} \cdot \sigma_{NO_2}(\lambda) - \sum_k b_k \lambda^k\right]^2 \tag{7.4}$$

This step is done by the fit routine in DOASIS.

1. Select a reference cross section which you want to fit to the measured signal.
   Click on the *Fitting* tab on the bottom of the screen (see figure 7.4). Double click on a line *Reference Name* column to add a reference. The reference cross section spectrum must be open in DOASIS.

2. Select an appropriate fit range. To do this, place the red *Fit Marker* (*View → Markers*) over the area of the spectrum that you want to fit. The *Fit Marker* can be moved and resized in the same way as the *Math Marker*.
   When selecting a wavelength range for your fit, try to keep the following aspects in mind:

   - As a general rule, the width of the fitting range should be < 50 nm.

   - *How is the saturation of your spectrum?* Don't include areas of the spectrum in which the saturation is low.

   - *Where are the largest differential absorption structures of the trace gas you want to evaluate?*

   - *What other trace gases must be taken into account in this wavelength range?* (In this case, the gas cell only contains NO_2, but in the atmosphere there will be several trace gases which absorb simultaneously.)

   To study these aspects, it can be helpful to compare your measurement with the reference cross section. First, save your measurement. Then, run a high pass filter over it (*Math → Filter → High Pass Binomial...*) to remove broadband structures. Do the same for the NO_2 cross section, and overlay the two spectra on top of each other. You should now be able to clearly see the NO_2 absorption in your gas cell. Find an appropriate fit range, then use the *Undo* function to undo the filtering (alternatively you can reload your saved spectra).
   Once you have found an appropriate fit range, you can enter this directly into the *Properties* window (*Marker → FitHigh, FitLow*) or use the red *Fit Marker* (*View → Markers → Show Fit Marker*) to select a range and then click on *Get* in the *Fitting* tab to automatically input the edges of the fit range into the fit scenario.

3. Select a DOAS-polynomial of 3rd to 5th order, in order to account for broad structures like the intensity variation of the lamp. (You can also add an Offset polynomial to correct for spectrometer stray light.)

4. Start the fit by clicking on the red exclamation button.

After performing the fit, the fit coefficient for which the minimal χ^2 was found is given in the *Fit Coeff.* column of the *Fitting* register. Since the spectra were prepared according to the above equations, the fit coefficient represents the column density $\rho_{NO_2} \cdot L$ and the unit is molec/cm^2. The *Shift* value is the amount of pixels the spectrum was shifted to obtain an optimum fit, the *Squeeze* value is the factor by which it was squeezed or stretched. These values should be close to 0 and 1, respectively.
Now take a look at the *Fit Residual* spectrum and the obtained χ^2 value.

What should Fit Residual *look like in the case of an ideal fit?*

Try varying the fit range. You can save the *Fit Result* page by using *Print* and selecting *Microsoft XPS Document Writer* as *Printer.* (Deactivate the *Print spectrum information* button, since it takes up too much space on your plot.) This is very useful if you want to show and compare the quality of your fits in your protocol or report.
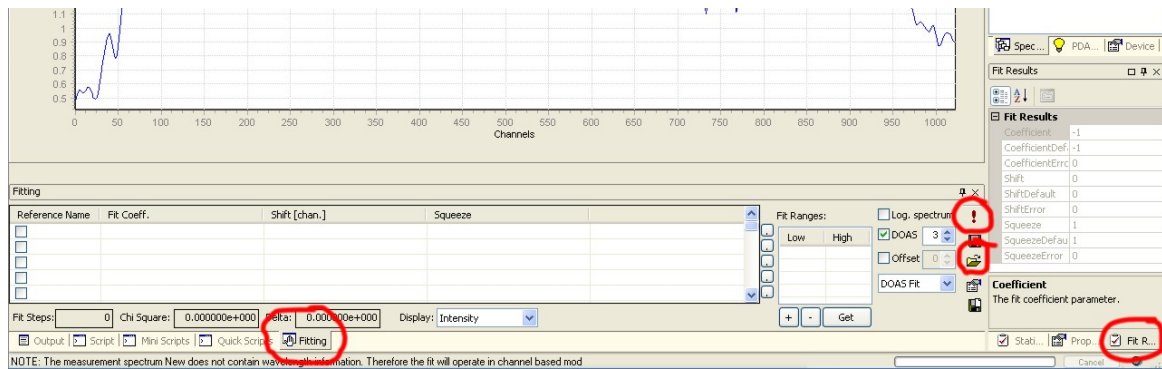
Figure 7.4: *The Fitting tab. The references are selected in the column* Reference Name. *Press* Get *to input the current edges of the* Fit Marker *into the fit settings. The exclamation point starts the fit. The disk button below it can be used to save the fit settings in a* Fit Scenario. Log. spectrum *takes the logarithm of the spectrum before doing the fit. It should be* **deactivated** *here as you already have taken the logarithm!*

When you have found the ideal fit range for this NO_2 measurement, take two new spectra of the halogen lamp and the gas cell, but this time optimize the saturation level (to about 80%) in this wavelength range. Rerun the fit.

Calculate the NO_2 concentration and the mixing ratio (amount NO_2 molecules per air molecule) in the gas cell assuming normal pressure and temperature.[3]
If you leave the lab now, remember to **CAREFULLY** reattach the fibre coupling to the fibres of the telescope on the roof. Check if the telescope points to the zenith, close DOASIS and start the program *Dauermessung* on the Desktop.

7.3   Atmospheric Measurements

In this section you will use the techniques you have learned to evaluate atmospheric measurement spectra recorded with this experimental setup. The instruments typically run in a zenith viewing direction, and it will be your task to evaluate the spectra from past measurements. First, you will evaluate ozone, then NO_2. For each species, you will calculate slant column densities as well as vertical columns. The approach will be to first evaluate a single measurement by means of which you will optimize the fit settings. These settings will then be saved in a *Fit Scenario* and will then be used to automatically evaluate the other spectra of that day. The final product of the evaluations will be a time series of the vertical and slant column densities for the entire day.

7.3.1   Configuring the fit with a single measurement

1. Pick a day to evaluate. The spectrometer usually runs all the time in zenith observation. You find the spectra in *FPDaten:\FP\Daten\Streulicht*. Choose a summer day with a few hundred spectra and store all spectra in both the *FP\aktuell\Streulicht* and the *FP\aktuell\Streulichtspektren* folders. Delete all spectra previously stored there. Find a midday (Fraunhofer reference) and evening spectrum from the day you wish to evaluate. To do this, open the logfile of your date in the *FPDaten:\FP\Logfiles* folder to find the *Fraunhofer reference*. The reference spectrum is the spectrum recorded at the smallest

---

[3]Avogadro's constant $= 6.022 \cdot 10^{23}$ Mol^{-1}, Molar volume $= 22{,}4 \; \frac{l}{Mol}$

solar zenith angle. Write down the spectrum number of this spectrum. Also find a spectrum recorded in the evening at a solar zenith angle close to 80° and write down the spectrum number. Open these two spectra, correct them for offset and dark current, and save them in your directory. If no logfile is available, have a look on the recording time of the spectra - this gives you a good hint on the solar zenith angle (SZA) at the time of recording. You can see the SZA in the *Properties* tab in DOASIS under *ScanGeometry* and then iterate to the reference spectrum. Note that the time stamp is UTC (consider this when choosing the starting time for your search).
Why is it advantageous to use a spectrum with a high solar zenith angle to optimize the settings for your fit?

2. Calculate the Ring Spectrum.
Open the *Fraunhofer reference* and add your wavelength calibration. Then use the menu entry *Math → Ring Spectrum* to calculate a Ring spectrum. Save the obtained spectrum. It will be used in the fit procedure to correct for the Ring effect.

3. *Tip:* Go back to the scattered light spectra. Make a copy of the evening spectrum, divide the *Fraunhofer reference* by it and calculate the optical density by taking the logarithm. You should now be able to see the structured absorption lines of ozone in the lower wavelength range, and probably also of NO_2 in the higher wavelength range. This should give you a good idea of the wavelength ranges where you can do the fit (see item 5 below). Save your optical density spectrum.

4. For the automated retrieval however, go back to your *Fraunhofer reference* and take the logarithm. Save this spectrum. Instead of dividing the *Fraunhofer reference* by the evening spectrum, we will now include the logarithm of the reference spectrum as a reference cross section in the fit. It needs to be input as the **first fit reference** in the fit scenario.[4]

5. Include your *Ring spectrum* in the fit scenario and link shift and squeeze of the Ring spectrum to the reference. Then open all convolved trace gas cross sections and include them in the fit scenario. It is advisable to link the shift and squeeze of all trace gases together (for example, link the shift and squeeze of NO2 and O4 to O3).

6. Make sure, the 'Log. Spectrum' option on the right is left open at any time. We take the logarithm of the measurement spectrum by hand later. Also the evaluation script takes the logarithm of the measurement spectra automatically.

   Why is this helpful to get realistic results?

7. Find appropriate wavelength ranges for ozone and for NO_2.

   What are the criteria for finding these fit ranges?

   Use the overlay function of DOASIS to compare your optical density spectrum to the

---

[4]Mathematically, fitting the logarithm of the *Fraunhofer reference* is the same as dividing by it as can be shown in the Beer-Lambert law (equation 4.6), except for one small difference: The fit now allows the spectrum to be slightly shifted against the measurement spectrum. This can be useful if the spectrometer's wavelength calibration is not perfectly stable during the course of the day. Strictly speaking, the fit coefficient of the logarithm of the *Fraunhofer reference* can be fixed to 1 (or -1, depending on the setup of the fit scenario). The automated retrieval script monitors the fit coefficient of the first reference spectrum, and gives a warning if it is not close to 1.

individual reference cross sections of ozone, NO$_2$, H$_2$O and O$_4$. Try to avoid wavelength regions in which the H$_2$O absorption is prominent, as removing these structures can be tricky.

8. Once you have found appropriate fit settings, select the evening spectrum in the spectrum sheet, take its logarithm and start the fit. Remember to include the reference cross sections of any species absorbing in your fit range as well as the Ring spectrum. Take a screenshot of the DOAS fit result overview tab in DOASIS for both the O$_3$ and NO$_2$ fits. *Compare your fit scenario with equation 4.8 and identify all terms, including the polynomials.*

9. Review the fit results. Ask yourself the following questions to assess the quality of the fit:

   - What does the fit residual look like?

   - Were the traces gases included in the fit identified?

   - What is the χ^2 value?

10. Play around with the fit settings until you are content that the configuration is correct and the fit quality is good.

11. Save your final fit settings in a *Fit Scenario* by clicking on the disk button below the exclamation point. Use the path *FPDaten:\FP\aktuell*. The file name must not exceed eight characters. **Check for a very last time, that the 'Log. Spectrum' option is left open before saving the fit szenario!**

7.3.2 Automated evaluation of an entire day

Now you will evaluate the spectra from the entire day using the settings you found for the evening spectrum. The script *AutomatischeAuswertung.js* in the directory
FPDaten:\FP\Daten\Scripts will help you. It uses your offset and dark current spectra to correct each individual measurement spectrum, then uses your *Fit Scenario* to subsequently run the fit for each spectrum. The fit results are stored in a text file.
The ozone evaluation is somewhat easier than the NO$_2$ retrieval. Therefore, it is best to start with ozone. Also, plot the fit results for ozone and make sure they are reasonable before starting the NO$_2$ evaluation. Reasonable means that you observe a U-shape.

1. Before you begin the automated retrieval, make sure your offset and dark current spectra are saved as *Offset.sp2* and *Dunkelstrom.sp2* in the directory
FPDaten:\FP\aktuell\Korrekturspektren. Also, your *Fit Scenario* needs to be in the directory *FPDaten:\FP\aktuell* and all spectra to be evaluated in both
FPDaten:\FP\aktuell\Streulicht and *FPDaten:\FP\aktuell\Streulichtspektren*.

2. Start *AutomatischeAuswertung.js*. The script will ask you for the following input: [5]

   - First, the script tells you to recheck your offset, dark current and fit scenario files. As you have already done this click the mouse in the next free line in the output window and press ENTER.

---

[5]WARNING: This script closes all open spectra in DOASIS, so be sure to save your data first. Also, the input window unfortunately does not accept the BACKSPACE or DEL keys. If you make a typing mistake you will need to start the script again from the beginning.

- Now the script asks for the name of your *Fit Scenario*. Type in the file name, but do not include the file extension *.fs. Press ENTER.

- Finally, the script asks for a name for the result text file. Choose a name with less than 8 characters, only include lower case letters and numbers and don't include a file extension. Press ENTER.

If all the information was entered correctly, the script now runs the evaluation. The χ^2 values are displayed in the output window along with any warnings that may occur.

3. Once the evaluation has finished, you can evaluate your result file stored in *FPDaten:\FP\aktuell*. Create the following plots:

   - Time series of the differential slant column density (dSCD) for ozone and NO$_2$

   - Langley Plot for ozone

   - Time series of the vertical column density (VCD) for Ozone in Dobson Units[6]

   What should the time series of ozone dSCDs look like? What about the VCD time series?

   What is the main difference between the ozone and NO$_2$ time series, and what causes this difference?

If you want to do a detailed evaluation at home, you should now quickly check if the output looks reasonable. One way to do this is by plotting the dSCD time series for both trace gases using Origin, which is installed on the computer outside the virtual machine. Choose plotting and select the time as the x-axis, and the fit coeffient as the y-axis. You would expect the time series to have a U-shape.

If you leave the lab now, remember to **CAREFULLY** reattach the fibre coupling to the fibres of the telescope on the roof. Check if the telescope points to the zenith, close DOASIS and start the program *Dauermessung* on the Desktop.

7.4 Multi Axis DOAS (MAX-DOAS)

The MAX-DOAS technique is used to gain insight into the vertical distribution of trace gases in the atmosphere. To this extent, scattered light spectra are recorded using different telescope elevation angles.

7.4.1 Recording scattered light spectra at different elevation angles

If possible, you should record 4 sets of MAX-DOAS measurements. Each set consists of three measurements at different telescope elevation angles. These three measurements should be conducted in rapid succession if possible. *Why is this important?* Make sure that the telescope is clean and that there is no water or ice in the tube:

- Measure a spectrum at 7° elevation.

- Measure a spectrum at 12° elevation.

- Measure a zenith spectrum at 90° elevation.

---

[6]1 DU = 2,6 $\cdot 10^{16} \frac{molecules}{cm^2}$.

Use the metal plate mounted on the telescope to adjust to the different elevation angles. Even though the telescope needs to be readjusted very often, please record the MAX-DOAS measurements in the order mentioned above: 7°, 12°, 90°, 7°, 12°, 90°, 7°, ... Be sure to adjust the exposure time of the spectrometer to obtain an appropriate saturation level for each individual spectrum. The individual spectra do **NOT** need to be recorded at the same exposure time. Take about 1000 exposures per spectrum. Note the weather conditions during the measurements to be able to better interpret your data later.

7.4.2 MAX-DOAS evaluation

1. Use the respective 90° spectra as your *Fraunhofer reference* spectrum for each set. Perform the necessary corrections and calculate a Ring spectrum.

2. Evaluate the individual MAX-DOAS spectra for ozone, NO_2, and O_4. Write down the individual fit coefficients of each target gas.

3. Plot your results with Python. How do the dSCDs of the individual species depend on the telescope elevation angle? How do they depend on the reference?

7.5   Before you leave...

- Adjust the telescope to the zenith position

- Close *DOASIS*

- Start *Dauermessung* on the Windows XP Desktop by double-clicking it.

- Remove any files you have added to *FPDaten:\FP\aktuell* and put them in your own folder for later reference.

Chapter 8

Course Report

Be sure to include the following points in your course report:

1. Characterizing the instrumentation

   - Offset and dark current (give average values)
   - Plot the dark current signal as a function of the exposure time. Is the dark current stable?
   - Plot the instrument noise and the total noise as a function of the number of exposures
   - Plot the noise of the optical density as a function of exposures
   - Compare the instrument noise to the total noise
   - Determine the wavelength calibration and the optical resolution of the spectrometer

2. Gas cell measurements

   - NO_2 concentration in the gas cell
   - NO_2 mixing ratio in the gas cell

3. Differential slant column densities for O_3 and NO_2

   - Plot ΔSCD for ozone and NO_2 as a function of time of day
   - What should these plots look like? Explain why.
   - Do these plots match your expectations? Give possible explanations for any discrepancies.

4. Langley Plot for ozone

   - Langley Plot: ΔSCD as a function of Air Mass Factor (AMF) for AMF < 5.
   - Determine the ozone reference slant column density SCD_{ref} in the Fraunhofer reference by extrapolating the Langley Plot for AMF < 3.5. Also estimate the error of this value by determining a maximum and minimum possible extrapolation in your data.

5. Plot the time series of the ozone vertical column density (VCD) over the course of the day. Include error bars. Compare your VCD to ozone data from satellite measurements. This data can be found at `http://ozoneaq.gsfc.nasa.gov`. Heidelberg is at longitude 8.49 and latitude 49.29.

6. MAX-DOAS

- Plot the ΔSCD as a function of the telescope elevation angle for ozone, NO_2 and O_4 for each set and compare the measurement sets.

- Which of these trace gases were found in the troposphere, which were only seen in the stratosphere?

- Can you see the influence of clouds in your O_4 measurements?

Please include a critical discussion of your results. Include possible explanations for unexpected results.

Bibliography

[1] Beirle, S., U. Platt, and T. Wagner (2004). Personal Communication. *Institute of Environmental Physics, Heidelberg.*

[2] Carroll, M. A. and A. Thompson (1995). Progress and Problems in Atmospheric Chemistry, Chapter NOx in the non-urban troposphere. *Singapore World Scientific.*

[3] Chapman, S. (1930). On ozone and atomic oxygen in the upper atmosphere. *Philos. Mag., Vol. 10, 369-383*

[4] Crutzen, P. (1970). The influence of nitrogen oxides on the atmospheric ozone content. *Quart. J. Roy. Meteor. Soc. 96, 320-325.*

[5] Czerny, M. und A. Turner (1930). *Z. Phys. 61,* 792

[6] Deutschmann, T. at al. (2011). The Monte Carlo atmospheric radiative transfer model McArtim: Introduction and validation of Jacobians and 3D features. *Journal of Quantitative Spectroscopy and Radiative Transfer, 112(6), 1119-1137.*

[7] Finlayson-Pitts, B. J. and J. N. Pitts (2000). Chemistry of the Upper and Lower Atmosphere. *San Diego: Academic Press.*

[8] Frieß, U. et al. (2006). MAX-DOAS O4 measurements: A new technique to derive information on atmospheric aerosols: 2. Modeling studies. *Journal of Geophysical Research: Atmospheres (1984?2012), 111(D14).*

[9] Frieß, U. et al. (2011). The vertical distribution of BrO and aerosols in the Arctic: Measurements by active and passive differential optical absorption spectroscopy. *Journal of Geophysical Research: Atmospheres (1984?2012), 116(D14).*

[10] General, S. et al. (2014). The Heidelberg Airborne Imaging DOAS Instrument (HAIDI) - A Novel Imaging DOAS Device for 2-D and 3-D Imaging of Trace Gases and Aerosols. *Submitted, Atmos. Meas. Tech.*

[11] Grainger, J. und J. Ring (1962). Anomalous Fraunhofer line profiles. *Nature 193,* 762

[12] Henriksen, T. et al. (1990). Ultraviolet-Radiation and skin cancer. Effect of an ozone layer depletion. *Photochemistry and photobiology, 51(5), 579-582.*

[13] Hönninger, G., Friedeburg, C. V. and Platt, U. (2004). Multi axis differential optical absorption spectroscopy (MAX-DOAS). *Atmospheric Chemistry and Physics, 4(1), 231-254.*

[14] Irie, H. et al. (2011). Eight-component retrievals from ground-based MAX-DOAS observations. *Atmos. Meas. Tech., 4, 1027-1044, doi:10.5194/amt-4-1027-2011.*

[15] Lee, D. et al. (1997). Estimations of global NOx emissions and their uncertainties. *Atmos. Environ. 31 (12), 1735-1749.*

[16] Leighton, P. (1961). Photochemistry of air pollution. *New York: Academic Press.*

[17] Levenberg, K. (1944). A Method for the Solution of Certain Non-Linear problems in Least Squares. *Q. Appl. Math., 2, 164-168.*

[18] Marquardt, D. W. (1963). An algorithm for the least-squares estimation of nonlinear parameters. *J. Appl. Math., 11, 431?441, doi:10.1137/0111030*

[19] Mentel, T., D. Bleilebens, and A. Wahner (1996). A study of nitrogen oxide oxidation in a large reaction chamber- the fate of NO2, N2O5, HNO3 and O3 at different humidities. *Atmos. Environ. 30, 4007-4020.*

[20] Parrish, D. D. et al. (1986). Measurements of the NOx-O3 photostationary state at Niwot Ridge, Colorado. *J. Geophys. Res. 91 (D5), 5361-5370.*

[21] Platt, U., D. Perner and H.W. Pätz (1979). Simultaneous measurement of Atmospheric CH_2O, O_3 and NO_2 by differential optical absorption. *J. Geophys. Res. 84, 6329-6335.*

[22] Platt, U. and J. Stutz (2008). Differential Optical Absorption Spectroscopy: Principles and Applications. Series: Physics of Earth and Space Environments, *Springer.*

[23] Prados-Roman, C. et al. (2011). Airborne DOAS limb measurements of tropospheric trace gas profiles: case studies on the profile retrieval of O4 and BrO. *Atmos. Meas. Tech., 4, 1241-1260, doi:10.5194/amt-4-1241-2011.*

[24] Press, W. H. et al. (1986). Numerical recipes: The art of scientific computing. *ISBN 0-521-43108-5, Cambridge University Press, Cambridge.*

[25] Rodgers, C. D. (2000). Inverse methods for atmospheric sounding. *World Scientific.*

[26] Roedel, W. (2011). Physik unserer Umwelt: Die Atmosphäre. *Springer Verlag.*

[27] Schulte, I. (2013). Electronic characterisation of the airborne HALO mini-DOAS instrument and recording and simulation of reference spectra. *Bachelor-Thesis, Institute of Environmental Physics, Heidelberg.*

[28] Slaper, H. et al. (1996). Estimates of ozone depletion and skin cancer incidence to examine the Vienna Convention achievements. *Nature, 384(6606), 256-258.*

[29] Smith, R. C. et al. (1992). Ozone depletion: ultraviolet radiation and phytoplankton biology in Antarctic waters. *Science, 255(5047), 952-959.*

[30] Trenberth, K. E., Fasullo, J. T., and Kiehl, J. (2009). Earth's global energy budget. *Bulletin of the American Meteorological Society*, 90(3).

[31] Trick, S. (2004). Formation of Nitrous Acid on Urban Surfaces. *Ph. D. thesis, University of Heidelberg.*

[32] Vountas, M., Rozanov, V. V., and Burrows, J. P. (1998). Ring effect: Impact of rotational Raman scattering on radiative transfer in Earth's atmosphere. *Journal of Quantitative Spectroscopy and Radiative Transfer, 60(6), 943-961.*

[33] Wagner, T. et al. (2004). MAX-DOAS O4 measurements: A new technique to derive information on atmospheric aerosols - Principles and information content. *J. Geophys. Res., 109, D22205, doi:10.1029/2004JD004904.*

[34] Wagner, T. et al. (2011): Inversion of tropospheric profiles of aerosol extinction and HCHO and NO2 mixing ratios from MAX-DOAS observations in Milano during the summer of 2003 and comparison with independent data sets. *Atmos. Meas. Tech., 4, 2685-2715, doi:10.5194/amt-4-2685-2011.*

[35] Weiler, C. S., and Penhale, P. A. (1994). Ultraviolet radiation in Antarctica: measurements and biological effects *(Vol. 62, pp. 1-257). American Geophysical Union.*

[36] WHO (2003). Health Aspects of Air Pollution with Particulate Matter, Ozone and Nitrogen Dioxide . In: *Report on WHO Working Group, Bonn, Germany, 13- 15 January 2003.* Copenhagen, Denmark. World Health Organization Regional Office Europe.

[37] Young, A. T. (1981). Rayleigh scattering. *Applied Optics, 20(4), 533-535.*

[38] Zel'dovich, Y. (1946). The oxidation of nitrogen in combustion and explosions. *Acta PhysioChemica USSR 21, 577-628.*